scientific data

OPEN

DATA DESCRIPTOR

Refractiveindex.info database of optical constants

Mikhail N. Polyanskiy

We introduce the *refractiveindex.info* database, a comprehensive open-source repository containing optical constants for a wide array of materials, and describe in detail the underlying dataset. This collection, derived from a meticulous compilation of data sourced from peer-reviewed publications, manufacturers' datasheets, and authoritative texts, aims to advance research in optics and photonics. The data is stored using a YAML-based format, ensuring integrity, consistency, and ease of access. Each record is accompanied by detailed metadata, facilitating a comprehensive understanding and efficient utilization of the data. In this descriptor, we outline the data curation protocols and the file format used for data records, and briefly demonstrate how the data can be organized in a user-friendly fashion akin to the books in a traditional library.

Background & summary

The complex index of refraction $\tilde{n} = n + ik$ is essential for understanding the optical properties of materials due to its close relation with the relative permittivity ε_r ($\varepsilon_r = \tilde{n}^2$ in the case of non-magnetic materials[1]). In this context, n is the phase velocity ratio of light in a vacuum to that in the material, representing refraction. The extinction coefficient k measures absorption. The absorption coefficient α can be expressed as $\alpha = 4\pi k/\lambda$, with λ representing the light's wavelength.

Accurately determining both n and k, and their chromatic dispersion, is crucial in science, engineering, and 3D artistic rendering. The intricate design of optical instruments, particularly those minimizing aberrations, depends heavily on understanding the $n(\lambda)$ function of transparent optical materials[2]. Cross-disciplinary efforts to characterize optical material properties have resulted in a wealth of datasets and analytical formulas, enhancing our grasp and utilization of optical constants.

Initiatives to amalgamate scattered information on optical constants resulted in seminal works like Palik's comprehensive compilation[3], offering structured and uniformly formatted data. Though monumental, the rapid advancement of technology and research methodologies signposted the need for a more dynamic, easily accessible repository of n and k values. This need intensified with the emergence of high-peak-power lasers, highlighting the critical role of the nonlinear refractive index, n_2, in decoding material behavior under intense light. n_2 characterizes the refractive index's variation with the optical field intensity I, expressed as $n = n_0 + n_2 I$, where n_0 is the refractive index at zero intensity.

The *refractiveindex.info* database emerged in response, offering a systematically organized, dynamic repository of optical constants. Since its inception in 2008, continuous enhancements have established it as a reliable resource, with the YAML-based file format ensuring data integrity and ease of access. The integration of the n_2 database in 2023 reaffirms our dedication to addressing modern challenges in optics and photonics.

The subsequent sections delve into the methods employed for collecting the data included in *refractiveindex.info*, detailing the file format used for storing data records and our approach to verifying dataset integrity. We then highlight the application aspects of this dataset, illustrated with an example of an interactive data browser, and conclude with a statement on data availability.

Methods

Data source clarification. It is pivotal to underscore that our work does not generate original experimental data. Instead, we create a comprehensive data repository, systematizing and cataloging existing optical constants published by others. This approach ensures a diverse and rich collection of verified data is readily accessible for various applications in a standardized format. As a result, this section does not describe experimental procedures but focuses on the methodologies employed in data collection and formatting.

Brookhaven National Laboratory, Accelerator Test Facility, Upton, NY, 11973, USA. e-mail: polyanskiy@bnl.gov

Data collection. Data on the optical properties of materials is aggregated from a variety of publicly accessible and credible sources, ensuring a wide range of optical constants is represented. The systematic collection process involves categorizing the data based on the type of material, its properties, and the source of information. The entire process is mostly manual due to the large variety of data sources and presentation methods. Below, we detail the steps typically undertaken to identify sources, extract data, and convert it into a unified format used in the data records.

1. Identification of data sources
   (a) Existing data collections: The initial sources for literature containing data on optical constants were published collections, such as those included in the Handbook of Optics[4]. The publications referenced therein constituted our initial list of data sources.
   (b) Cross-references from the initial list of data sources: In the next iteration, we scan for references to other publications in the sources identified in the previous step (usually, scientific papers reporting new measurements describe previous works on similar topics).
   (c) Search engines: We perform a broader search for publications on optical properties of materials using tools like Google Scholar to find newer references and those that may have been missed in earlier steps.
   (d) Glass makers' catalogs: We checked the websites of glass manufacturers for catalogs of glasses they produce. These catalogs are often available in Zemax AGF format, suitable for automatic data extraction.
   (e) User input: At the present maturity level of the project, most new data sources are recommended by users. Researchers often provide us with data in a format ready-to-include in the *refractiveindex.info* dataset as soon as the data are first published.

2. Data extraction
   (a) Dispersion formula: When the linear refractive index as a function of wavelength is given as a dispersion formula, the coefficients are manually transferred to the data record. Adjustments are made if necessary to fit the formula to one of the standard forms documented in the following section.
   (b) Tabulated numerical data: In cases where optical constants are presented in tabulated numerical form, the data are transferred to the data record with minimal changes required by the used format (e.g., using micrometer as the unit of wavelength and expressing internal absorption by extinction coefficient k). This process is simplified if data is in a standard table format (e.g., CSV or Microsoft Excel) in supplementary materials or directly provided by authors. For older publications, typically available as bitmap-based PDF files, text recognition options in PDF reading software prove helpful.
   (c) Models: If a reference presents a model for calculating optical constants, a Python script is developed to generate a tabulated data record compatible with the required format. This script is then made publicly available to *refractiveindex.info* users on GitHub.
   (d) Graphical-only data: Occasionally, authors choose to include only graphical data in publications without numerical data. In such cases, we first attempt to contact the authors for the original data. If this is not feasible (in the case of older publications) or if there is no response, semi-automatic digitization of the plots is sometimes performed (e.g., using Engauge Digitizer software); however, this is considered a last resort due to its time-consuming and less accurate nature and is typically used only when no alternative data is available.
   (e) Glass catalogs: Glass makers' catalogs in AGF format are automatically converted into *refractiveindex.info* data records using a dedicated Python script.

Data formatting and updates. All collected data are converted into a standardized format stored in human-readable YAML files, as detailed in the following section. This approach ensures consistency and facilitates easy access and manipulation by both users and computer programs.

Errors in converting original data to standardized data records occasionally occur and are typically reported by users. All efforts are made to implement necessary corrections promptly via regular updates of the dataset.

Data Records

The dataset is available at *Figshare*[5].

YAML-based file format for data records. The data records employ YAML-based file format (https://yaml.org), ensuring the data is both easily readable and maintainable. Each YAML file encompasses data related to a specific material, evaluated under defined conditions and reported in a particular publication, with a primary focus on the refractive index and extinction coefficient.

As an illustrative example, consider a data record for SiO_2 in which the refractive index n is expressed through a dispersion formula. The associated YAML file is located at `data-nk/main/SiO2/Malitson.yml` and is organized as follows:

```
REFERENCES: "1) I. H. Malitson, J. Opt. Soc. Am. 55, 1205-1209 (1965)...
COMMENTS: "Fused silica, 20°C"
DATA:
  - type: formula 1
    wavelength_range: 0.21 6.7
    coefficients: 0 0.6961663 0.0684043 0.4079426...
```

```
SPECS:
    n_is_absolute: false
    wavelength_is_vacuum: false
    temperature: 20°C
```

Every YAML data file primarily consists of two mandatory fields: REFERENCES and DATA. REFERENCES cite the source of the data, while DATA provides the values of the optical constants. There are also two optional fields, COMMENTS and SPECS, offering additional context and structured information respectively.

DATA. In the case of a data record for linear optical constants, the DATA field can be specified as a dispersion formula, identified by a formula number, or as tabulated data sets of $n(\lambda)$ and/or $k(\lambda)$. For dispersion formulas, the 'wavelength_range' entry indicates the applicable wavelength range for the data, always expressed in micrometers. Each dispersion formula in the database is numerically identified and described as follows:

$$n^2 - 1 = C_1 + \frac{C_2\lambda^2}{\lambda^2 - C_3^2} + \frac{C_4\lambda^2}{\lambda^2 - C_5^2} + \frac{C_6\lambda^2}{\lambda^2 - C_7^2} + \frac{C_8\lambda^2}{\lambda^2 - C_9^2} + \frac{C_{10}\lambda^2}{\lambda^2 - C_{11}^2} + \frac{C_{12}\lambda^2}{\lambda^2 - C_{13}^2} + \frac{C_{14}\lambda^2}{\lambda^2 - C_{15}^2} + \frac{C_{16}\lambda^2}{\lambda^2 - C_{17}^2} \tag{1}$$

$$n^2 - 1 = C_1 + \frac{C_2\lambda^2}{\lambda^2 - C_3} + \frac{C_4\lambda^2}{\lambda^2 - C_5} + \frac{C_6\lambda^2}{\lambda^2 - C_7} + \frac{C_8\lambda^2}{\lambda^2 - C_9} + \frac{C_{10}\lambda^2}{\lambda^2 - C_{11}} + \frac{C_{12}\lambda^2}{\lambda^2 - C_{13}} + \frac{C_{14}\lambda^2}{\lambda^2 - C_{15}} + \frac{C_{16}\lambda^2}{\lambda^2 - C_{17}} \tag{2}$$

$$n^2 = C_1 + C_2\lambda^{C_3} + C_4\lambda^{C_5} + C_6\lambda^{C_7} + C_8\lambda^{C_9} + C_{10}\lambda^{C_{11}} + C_{12}\lambda^{C_{13}} + C_{14}\lambda^{C_{15}} + C_{16}\lambda^{C_{17}} \tag{3}$$

$$n^2 = C_1 + \frac{C_2\lambda^{C_3}}{\lambda^2 - C_4^{C_5}} + \frac{C_6\lambda^{C_7}}{\lambda^2 - C_8^{C_9}} + C_{10}\lambda^{C_{11}} + C_{12}\lambda^{C_{13}} + C_{14}\lambda^{C_{15}} + C_{16}\lambda^{C_{17}} \tag{4}$$

$$n = C_1 + C_2\lambda^{C_3} + C_4\lambda^{C_5} + C_6\lambda^{C_7} + C_8\lambda^{C_9} + C_{10}\lambda^{C_{11}} \tag{5}$$

$$n - 1 = C_1 + \frac{C_2}{C_3 - \lambda^{-2}} + \frac{C_4}{C_5 - \lambda^{-2}} + \frac{C_6}{C_7 - \lambda^{-2}} + \frac{C_8}{C_9 - \lambda^{-2}} + \frac{C_{10}}{C_{11} - \lambda^{-2}} \tag{6}$$

$$n = C_1 + \frac{C_2}{\lambda^2 - 0.028} + C_3\left(\frac{1}{\lambda^2 - 0.028}\right)^2 + C_4\lambda^2 + C_5\lambda^4 + C_6\lambda^6 \tag{7}$$

$$\frac{n^2 - 1}{n^2 + 2} = C_1 + \frac{C_2\lambda^2}{\lambda^2 - C_3} + C_4\lambda^2 \tag{8}$$

$$n^2 = C_1 + \frac{C_2}{\lambda^2 - C_3} + \frac{C_4(\lambda - C_5)}{(\lambda - C_5)^2 + C_6} \tag{9}$$

In another example, found at `data-nk/main/Si/Aspnes.yml`, $n(\lambda)$ and $k(\lambda)$ for Silicon (Si) are provided in tabulated numerical form:

```
DATA:
  - type: tabulated nk
      data: |
      0.2066 1.010 2.909
      0.2101 1.083 2.982...
```

Here, the first column corresponds to the wavelength in micrometers, while the others represent the unitless refractive index n and extinction coefficient k. Alternatively, n and k can be outlined separately in two two-column entries. A data entry might also combine a dispersion formula for n with numerical data for k, as illustrated in the SCHOTT N-BK7 glass dataset at `data-nk/glass/schott/N-BK7.yml`:

```
DATA:
  - type: formula 2
    wavelength_range: 0.3 2.5
    coefficients: 0 1.03961212 0.00600069867 0.231792344...
  - type: tabulated k
    data: |
    0.300 2.8607E-06
    0.310 1.3679E-06
    0.320 6.6608E-07
    ...
```

In n_2 datasets, the data are always presented numerically. An example can be found at `data-n2/main/SiO2/Flom.yml`. n_2 is expressed in m^2/W:

```
DATA:
  - type: tabulated n2
    data: |
        0.772 2.07e-20
        1.030 2.23e-20
        1.550 2.42e-20
SPECS:
    n2_method: Z-scan
    pulse_duration: 280e-15 140e-15 97e-15
```

It is noteworthy that for n_2, information on the measurement method and pulse duration is essential for comparing data from different sources. This information is specified in the optional SPECS field.

COMMENTS and SPECS. The COMMENTS field can incorporate additional information to provide context to the data, while the SPECS field presents structured data in key-value pairs, giving machine-interpretable insights into specific measurement conditions or additional properties.

In the initial example, the SPECS entries clarify that the refractive index is not absolute and is measured relative to air, that the wavelength is gauged under atmospheric conditions rather than in vacuum, and that the data is applicable at a temperature of 20 °C. In the preceding example concerning n_2, the SPECS delineate the use of the Z-scan measurement method, specifying pulse durations of 280 fs, 140 fs, and 97 fs for the corresponding data points. Furthermore, the SPECS section is adaptable to encapsulate an enhanced depth of information regarding the material, as illustrated in the forthcoming example for SCHOTT N-BK7 glass:

```
SPECS:
    ...
    thermal_dispersion:
      - type: "Schott formula"
        coefficients: 1.86e-06 1.31e-08 -1.37e-11 4.34e-07 6.27e-10 0.17
    nd: 1.5168
    Vd: 64.17
    glass_code: 517642.251
    glass_status: standard
    ...
    acid_resistance: 1.0
    alkali_resistance: 2.3
    phosphate_resistance: 2.3
```

Inclusion of additional information on optical glasses makes the data records suitable for use in optical design software.

Notes on data records. Adhering strictly to the syntactical rules of YAML is paramount. This adherence includes the mandatory use of spaces for indentation (tabs are prohibited) and the application of UTF-8 encoding without BOM, ensuring consistency and readability across diverse data records. While not a stringent requirement, a uniform format for similar entries, particularly references, is encouraged to optimize the user experience and enhance data interpretability.

Unless explicitly defined, non-prefixed SI units (e.g., watts, meters, seconds) are the default to ensure unambiguous and standardized data representation and interpretation. For instance, n_2 is expressed in units of m^2/W. However, an exception exists for the wavelength, which is always specified in micrometers to comply with a general practice accepted in optical design and, in particular, to allow the direct use of published dispersion formulas that traditionally assume wavelength expressed in micrometers.

Technical Validation

Since the described dataset[5] represents an extensive array of data compiled by the work of thousands of researchers over more than a century, we cannot verify the accuracy of every individual record. Instead, we rely on the peer-review process employed by publishers of scientific and technical journals, and on the experience and reputation of optical material manufacturers publishing their material properties. However, we make every effort to ensure the correctness of the data extraction and conversion process, as well as the consistency of the information included in the dataset. In particular, the following steps are typically involved in the process of adding a new data record.

1. Verification and documentation of data attribution: We trace the origin of the data to the first publication where it appeared and include the corresponding information in the data record file, ensuring users can validate the origins of the data. If the original data were re-analyzed, or a combination of data from multiple sources was used in a later publication (for example, to produce a dispersion formula valid in an extended wavelength range), this fact is also documented in the REFERENCES field of the data record file.
2. Verification of accuracy of data extraction: Several tests are used to ensure the absence of errors in the conversion process:
   (a) Manual number-by-number comparison: This test is routinely performed when the data is represented by a relatively small amount of numerical values, e.g., coefficients of a dispersion formula.
   (b) Plot comparison: We use Python scripts that automatically read YAML data record files and plot the included optical constants as a function of wavelength. Comparing these plots with those included in the original publications is a robust tool for spotting inconsistencies.
   (c) Looking for data abnormalities: A deviation of a data point from the general trend in the data record is usually an indication of a data extraction error. All such abnormalities are manually compared against the original data, and necessary corrections are made.
   (d) Cross-entry comparison: Plotting data entries for the same material from different sources on the same plot may help reveal a systematic error in a particular data record if a corresponding curve deviates from a general trend. An example of a Python-based user interface allowing for easy data comparison is given in the following section.
3. Testing of data file adherence to the YAML standard: This is typically performed by verifying the as-expected operation of several scripts used to access the data and relying on standardized YAML processing libraries. Error or warning messages generated by these scripts indicate a problem in the data record file that must be identified and corrected.
4. User feedback: This is our strongest defense line in assuring the integrity of the data records. The users report errors via the GitHub page of the *refractiveindex.info* project or by directly contacting the maintainer. Each report is analyzed, and necessary corrections are promptly implemented.

Usage Notes

The described dataset[5] is a collection of human-readable YAML files, meticulously organized for user convenience. While these files can be directly individually accessed for specific optical constants of materials, organizing them in a logically-structured way and employing computer programs for data retrieval and analysis unleashes the dataset's comprehensive utility. The YAML format, a standardized data serialization language, ensures that the data files are easily parsable with libraries such as PyYAML for Python and libyaml for C/C++.

The *refractiveindex.info* database is build upon the dataset described in the previous sections and include additions aimed at simplifying the access and navigation through the data. The main addition is a descriptor defining a hierarchical structure akin to a library. In this setup, each data record is akin to a "page," housed within a "book," and all such books are systematically arranged on different "shelves." This logical structure is defined and maintained through YAML-based catalog files, that categorize each data record following the 'library' analogy and indicate the relative path of the corresponding data records.

The library is defined by two catalog files: `catalog-nk.yml` for linear optical properties and `catalog-n2.yml` for nonlinear properties. Below is an excerpt from the `catalog-n2.yml file`, exemplifying the integration of HTML typesetting and showcasing optional entries like 'DIVIDER' and 'info'. The 'DIVIDER' is employed to separate distinct groups of books or pages clearly, while 'info' links to an HTML file furnishing extra details about a particular shelf, book, or page.

```
- SHELF: main
  name: "MAIN - simple inorganic materials"
  content:
    - DIVIDER: "Al - Aluminates, Aluminium garnets"
    - BOOK: BeAl2O4
      name: "BeAl2O4 (Beryllium aluminate, chrysoberyl)"
      info: "main/BeAl2O4.html"
      content:
        - PAGE: Adair
          name: "Adair 1989"
          data: "main/BeAl2O4/Adair.yml"
    ...
```

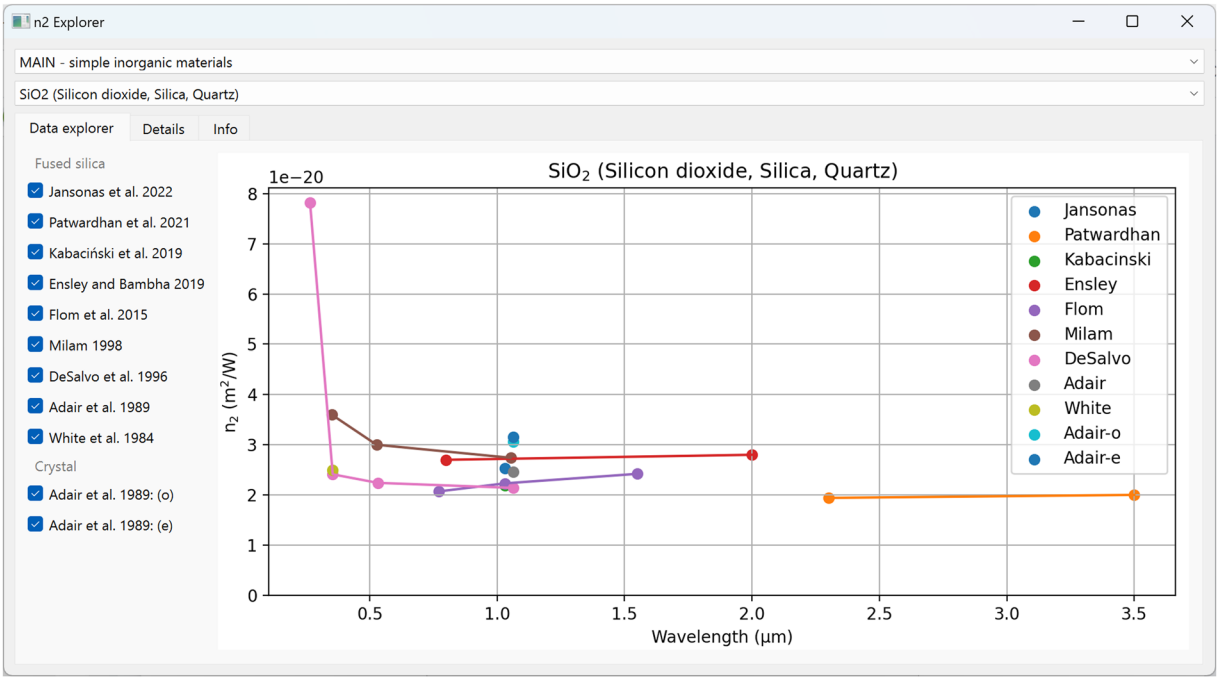

Fig. 1 The `n2explorer.py` script's graphical user interface facilitates visual navigation through the n_2 data. The `nkexplorer.py` script provides a similar interface for exploring linear optical constants.

```
- BOOK: MgAl2O4
  name: "MgAl2O4 (Magnesium aluminate, spinel)"
  info: "main/MgAl2O4.html"
  content:
    - PAGE: Flom
      name: "Flom et al. 2015"
      data: "main/MgAl2O4/Flom.yml"
    - PAGE: Adair
      name: "Adair et al. 1989"
      data: "main/MgAl2O4/Adair.yml"
...
```

In this schema:

- 'SHELF' represents a specific category or collection of materials.
- 'BOOK' denotes a particular material.
- 'PAGE' entries detail individual data records associated with a material.
- 'DIVIDER' assists in visually and logically separating related materials or data records, enhancing the navigation experience.

The 'info' entry specifies paths to additional HTML-based information, enabling users to access in-depth insights. Each 'PAGE' entry is linked with a 'data' field, pointing to the exact location of the data record's YAML file within the dataset. The 'name' entry provides a "long" name for a shelf, book, or page in HTML typesetting. Paths to the data files for the linear (*nk*) and nonlinear (n_2) subsets of the database, as well as to the HTML files with additional information (*info*), are relative to the `data-nk`, `data-n2`, and `info` directories, respectively, all located in the database's root directory.

It's important to note that users can create alternative 'catalog' files tailored to their specific needs. For instance, a customized catalog can contain only a subset of the dataset that is relevant for a particular application or study.

To aid users in navigating the data, two Python scripts, `nkexplorer.py` and `n2explorer.py`, are housed in the `tools` folder in the root directory of the *refractiveindex.info* database. These utilities, boasting a QT-based graphical interface, facilitate the location and comparison of data from a variety of sources. Figure 1 displays the `n2explorer.py` interface, illustrating the visual comparison of n_2 data for SiO_2 sourced from multiple publications.

Furthermore, users have the option to access the database through the RefractiveIndex.INFO website (https://refractiveindex.info). This online platform facilitates the browsing of data records and computations of various optical properties linked with *n* and *k* constants, such as Abbe numbers, reflectance, and Brewster's angle.

A variety of third-party scripts and web applications that harness the *refractiveindex.info* dataset can be found, notably on GitHub. These tools offer users alternative avenues to efficiently access and employ the data.

Code availability

The dataset described here, which represents the core of the *refractiveindex.info* database, is available at *Figshare*[5]. It presently (as of December 2023) contains 3135 data records on 605 materials in the part of the dataset corresponding to linear optical properties (*nk*), and 193 records on 89 materials in the part corresponding to nonlinear optical properties (n_2).

The code that underpins the *refractiveindex.info* database is made accessible under the Creative Commons Zero (CC0) license (https://creativecommons.org/publicdomain/zero/1.0). This license facilitates the unrestricted use, distribution, and modification of the code, making it widely accessible for various applications. The entire codebase, including detailed documentation, is publicly available on the *refractiveindex.info-database* GitHub project (https://github.com/polyanskiy/refractiveindex.info-database). This repository is regularly updated, ensuring it evolves to meet the ongoing needs of both the scientific and engineering sectors. For additional utility, users can explore the *refractiveindex.info-scripts* project on GitHub (https://github.com/polyanskiy/refractiveindex.info-scripts), which offers scripts for deriving optical constants from established models and tools for converting Zemax glass catalogs to the dataset's YAML format.

It is essential to note that the data encapsulated within the *refractiveindex.info* dataset is meticulously curated from publicly available sources. This includes peer-reviewed journals, authoritative books, and manufacturer datasheets, ensuring that the dataset is not only expansive but also anchored in reliability and veracity. Each data record within the dataset explicitly cites the source, offering users a pathway to delve deeper into the original data and its context. All journal papers from which data are presently used in the *refractiveindex.info* dataset, excluding those without a DOI identifier, are included in the following reference list[6–471].

By integrating a comprehensive data collection, adopting a standard-based data file format, ensuring ongoing updates, and maintaining open access, the *refractiveindex.info* emerges as an essential tool for researchers, engineers, and students delving into the complex world of optical constants and material properties.

Received: 9 October 2023; Accepted: 27 December 2023;
Published online: 18 January 2024

References

1. Born, M. & Wolf, E. *Principles of optics* (Cambridge University Press, Cambridge, 1999).
2. Smith, W. J. *Modern Optical Engineering* (McGraw-Hill, New York, 2007).
3. Palik, E. D. (ed.) *Handbook of Optical Constants of Solids* (Academic Press, San Diego, 1998).
4. Bass, M. *et al.* (eds). *Handbook of Optics, Volume IV: Optical Properties of Materials, Nonlinear Optics, Quantum Optics*. (McGraw-Hill, New York, 2009).
5. Polyanskiy, M. N. *refractiveindex.info* data set. *Figshare*, https://doi.org/10.6084/m9.figshare.c.6868000.v1 (2024).
6. Adachi, S. Optical dispersion relations for GaP, GaAs, GaSb, InP, InAs, InSb, $Al_xGa_{1-x}As$, and $In_{1-x}Ga_xAs_yP_{1-y}$. *Journal of Applied Physics* **66**, 6030–6040, https://doi.org/10.1063/1.343580 (1989).
7. Adachi, S. Optical dispersion relations for AlSb from E=0 to 6.0 eV. *Journal of Applied Physics* **67**, 6427–6431, https://doi.org/10.1063/1.345115 (1990).
8. Adachi, S. & Taguchi, T. Optical properties of ZnSe. *Physical Review B* **43**, 9569–9577, https://doi.org/10.1103/physrevb.43.9569 (1991).
9. Adachi, S., Kimura, T. & Suzuki, N. Optical properties of CdTe: Experiment and modeling. *Journal of Applied Physics* **74**, 3435–3441, https://doi.org/10.1063/1.354543 (1993).
10. Adair, R., Chase, L. L. & Payne, S. A. Nonlinear refractive-index measurements of glasses using three-wave frequency mixing. *Journal of the Optical Society of America B* **4**, 875, https://doi.org/10.1364/josab.4.000875 (1987).
11. Adair, R., Chase, L. L. & Payne, S. A. Nonlinear refractive index of optical crystals. *Physical Review B* **39**, 3337–3350, https://doi.org/10.1103/physrevb.39.3337 (1989).
12. Afsar, M. N. & Hasted, J. B. Measurements of the optical constants of liquid H_2O and D_2O between 6 and 450 cm^{-1}. *Journal of the Optical Society of America* **67**, 902, https://doi.org/10.1364/josa.67.000902 (1977).
13. Aftenieva, O. *et al*. Lasing by template-assisted self-assembled quantum dots. *Advanced Optical Materials* **11**, https://doi.org/10.1002/adom.202202226 (2023).
14. Aftenieva, O. *et al.* Directional amplified photoluminescence through large-area perovskite-based metasurfaces. *ACS Nano* **17**, 2399–2410, https://doi.org/10.1021/acsnano.2c09482 (2023).
15. Aguilar, O., de Castro, S., Godoy, M. P. F. & Rebello Sousa Dias, M. Optoelectronic characterization of $Zn_{1-x}Cd_xO$ thin films as an alternative to photonic crystals in organic solar cells. *Optical Materials Express* **9**, 3638, https://doi.org/10.1364/ome.9.003638 (2019).
16. Harasaki, A. & Kato, K. New data on the nonlinear optical constant, phase-matching, and optical damage of $AgGaS_2$. *Japanese Journal of Applied Physics* **36**, 700, https://doi.org/10.1143/jjap.36.700 (1997).
17. Al-Kuhaili, M. Optical properties of hafnium oxide thin films and their application in energy-efficient windows. *Optical Materials* **27**, 383–387, https://doi.org/10.1016/j.optmat.2004.04.014 (2004).
18. Althoff, R. & Hertz, J. Measurement of the optical constants of Na and K in the range of wavelength from 2.5 to 10 μ. *Infrared Physics* **7**, 11–16, https://doi.org/10.1016/0020-0891(67)90025-5 (1967).
19. Amotchkina, T., Trubetskov, M., Hahner, D. & Pervak, V. Characterization of e-beam evaporated Ge, YbF_3, ZnS, and LaF_3 thin films for laser-oriented coatings. *Applied Optics* **59**, A40, https://doi.org/10.1364/ao.59.000a40 (2019).
20. Arakawa, E. T., Williams, M. W. & Inagaki, T. Optical properties of arc-evaporated carbon films between 0.6 and 3.8 eV. *Journal of Applied Physics* **48**, 3176–3177, https://doi.org/10.1063/1.324057 (1977).
21. Arakawa, E. T., Williams, M. W., Ashley, J. C. & Painter, L. R. The optical properties of kapton: Measurement and applications. *Journal of Applied Physics* **52**, 3579–3582, https://doi.org/10.1063/1.329140 (1981).
22. Arndt, D. P. *et al*. Multiple determination of the optical constants of thin-film coating materials. *Applied Optics* **23**, 3571, https://doi.org/10.1364/ao.23.003571 (1984).
23. Arosa, Y. & de la Fuente, R. Refractive index spectroscopy and material dispersion in fused silica glass. *Optics Letters* **45**, 4268, https://doi.org/10.1364/ol.395510 (2020).

24. Aspnes, D. E. & Studna, A. A. Dielectric functions and optical parameters of Si, Ge, GaP, GaAs, GaSb, InP, InAs, and InSb from 1.5 to 6.0 eV. *Physical Review B* **27**, 985–1009, https://doi.org/10.1103/physrevb.27.985 (1983).
25. Aspnes, D. E., Kelso, S. M., Logan, R. A. & Bhat, R. Optical properties of $Al_xGa_{1-x}As$. *Journal of Applied Physics* **60**, 754–767, https://doi.org/10.1063/1.337426 (1986).
26. Bååk, T. Silicon oxynitride; a material for GRIN optics. *Applied Optics* **21**, 1069, https://doi.org/10.1364/ao.21.001069 (1982).
27. Börzsönyi, A., Heiner, Z., Kalashnikov, M. P., Kovács, A. P. & Osvay, K. Dispersion measurement of inert gases and gas mixtures at 800 nm. *Applied Optics* **47**, 4856, https://doi.org/10.1364/ao.47.004856 (2008).
28. Babar, S. & Weaver, J. H. Optical constants of cu, ag, and au revisited. *Applied Optics* **54**, 477, https://doi.org/10.1364/ao.54.000477 (2015).
29. Ball, J. M. *et al*. Optical properties and limiting photocurrent of thin-film perovskite solar cells. *Energy & Environmental Science* **8**, 602–609, https://doi.org/10.1039/c4ee03224a (2015).
30. Barker, A. S. & Ilegems, M. Infrared lattice vibrations and free-electron dispersion in GaN. *Physical Review B* **7**, 743–750, https://doi.org/10.1103/physrevb.7.743 (1973).
31. Barnes, N. P. & Piltch, M. S. Temperature-dependent Sellmeier coefficients and nonlinear optics average power limit for germanium. *Journal of the Optical Society of America* **69**, 178, https://doi.org/10.1364/josa.69.000178 (1979).
32. Barnes, N. P. & Gettemy, D. J. Temperature variation of the refractive indices of yttrium lithium fluoride. *Journal of the Optical Society of America* **70**, 1244, https://doi.org/10.1364/josa.70.001244 (1980).
33. Bassarab, V. V., Shalygin, V. A., Shakhmin, A. A., Sokolov, V. S. & Kropotov, G. I. Spectroscopy of a borosilicate crown glass in the wavelength range of 0.2 μm–15 cm. *Journal of Optics* **25**, 065401, https://doi.org/10.1088/2040-8986/accaf9 (2023).
34. Beadie, G., Brindza, M., Flynn, R. A., Rosenberg, A. & Shirk, J. S. Refractive index measurements of poly(methyl methacrylate) (PMMA) from 0.4—1.6 μm. *Applied Optics* **54**, F139, https://doi.org/10.1364/ao.54.00f139 (2015).
35. Beaini, R., Baloukas, B., Loquai, S., Klemberg-Sapieha, J. & Martinu, L. Thermochromic VO_2-based smart radiator devices with ultralow refractive index cavities for increased performance. *Solar Energy Materials and Solar Cells* **205**, 110260, https://doi.org/10.1016/j.solmat.2019.110260 (2020).
36. Beal, A. R. & Hughes, H. P. Kramers-Kronig analysis of the reflectivity spectra of 2H-MoS_2, 2H-$MoSe_2$ and 2H-$MoTe_2$. *Journal of Physics C: Solid State Physics* **12**, 881–890, https://doi.org/10.1088/0022-3719/12/5/017 (1979).
37. Beliaev, L. Y., Shkondin, E., Lavrinenko, A. V. & Takayama, O. Thickness-dependent optical properties of aluminum nitride films for mid-infrared wavelengths. *Journal of Vacuum Science & Technology A: Vacuum, Surfaces, and Films* **39**, https://doi.org/10.1116/6.0000884 (2021).
38. Beliaev, L. Y., Shkondin, E., Lavrinenko, A. V. & Takayama, O. Optical, structural and composition properties of silicon nitride films deposited by reactive radio-frequency sputtering, low pressure and plasma-enhanced chemical vapor deposition. *Thin Solid Films* **763**, 139568, https://doi.org/10.1016/j.tsf.2022.139568 (2022).
39. Beliaev, L. Y., Shkondin, E., Lavrinenko, A. V. & Takayama, O. Erratum: "Thickness-dependent optical properties of aluminum nitride films for mid-infrared wavelengths" [J. Vac. Sci. Technol. A 39, 043408 (2021)]. *Journal of Vacuum Science & Technology A* **40**, https://doi.org/10.1116/6.0001574 (2022).
40. Beliaev, L. Y., Shkondin, E., Lavrinenko, A. V. & Takayama, O. Optical properties of plasmonic titanium nitride thin films from ultraviolet to mid-infrared wavelengths deposited by pulsed-DC sputtering, thermal and plasma-enhanced atomic layer deposition. *Optical Materials* **143**, 114237, https://doi.org/10.1016/j.optmat.2023.114237 (2023).
41. Belosludtsev, A. *et al*. Correlation between stoichiometry and properties of scandium oxide films prepared by reactive magnetron sputtering. *Applied Surface Science* **427**, 312–318, https://doi.org/10.1016/j.apsusc.2017.08.068 (2018).
42. Bertie, J. E., Lan, Z., Jones, R. N. & Apelblat, Y. Infrared intensities of liquids XVIII: Accurate optical constants and molar absorption coefficients between 6500 and 800 cm^{-1} of dichloromethane at 25 °C, from spectra recorded in several laboratories. *Applied Spectroscopy* **49**, 840–851, https://doi.org/10.1366/0003702953964435 (1995).
43. Bhar, G. C. Refractive index interpolation in phase-matching. *Applied Optics* **15**, 305, https://doi.org/10.1364/ao.15.0305_1 (1976).
44. Bhar, G. C. & Ghosh, G. Temperature-dependent Sellmeier coefficients and coherence lengths for some chalcopyrite crystals. *Journal of the Optical Society of America* **69**, 730, https://doi.org/10.1364/josa.69.000730 (1979).
45. Bideau-Mehu, A., Guern, Y., Abjean, R. & Johannin-Gilles, A. Interferometric determination of the refractive index of carbon dioxide in the ultraviolet region. *Optics Communications* **9**, 432–434, https://doi.org/10.1016/0030-4018(73)90289-7 (1973).
46. Bideau-Mehu, A., Guern, Y., Abjean, R. & Johannin-Gilles, A. Measurement of refractive indices of neon, argon, krypton and xenon in the 253.7—140.4 nm wavelength range. dispersion relations and estimated oscillator strengths of the resonance lines. *Journal of Quantitative Spectroscopy and Radiative Transfer* **25**, 395–402, https://doi.org/10.1016/0022-4073(81)90057-1 (1981).
47. Bieniewski, T. M. & Czyzak, S. J. Refractive indexes of single hexagonal ZnS and CdS crystals. *Journal of the Optical Society of America* **53**, 496, https://doi.org/10.1364/josa.53.000496 (1963).
48. Birkhoff, R. D., Painter, L. R. & Heller, J. M. Optical and dielectric functions of liquid glycerol from gas photoionization measurements. *The Journal of Chemical Physics* **69**, 4185–4188, https://doi.org/10.1063/1.437098 (1978).
49. Bliss, E. S., Speck, D. R. & Simmons, W. W. Direct interferometric measurements of the nonlinear refractive index coefficient n_2 in laser materials. *Applied Physics Letters* **25**, 728–730, https://doi.org/10.1063/1.1655378 (1974).
50. Boidin, R., Halenkovič, T., Nazabal, V., Beneš, L. & Němec, P. Pulsed laser deposited alumina thin films. *Ceramics International* **42**, 1177–1182, https://doi.org/10.1016/j.ceramint.2015.09.048 (2016).
51. Bond, W. L. Measurement of the refractive indices of several crystals. *Journal of Applied Physics* **36**, 1674–1677, https://doi.org/10.1063/1.1703106 (1965).
52. Bond, W. L., Boyd, G. D. & Carter, H. L. Refractive indices of HgS (cinnabar) between 0.62 and 11 μ. *Journal of Applied Physics* **38**, 4090–4091, https://doi.org/10.1063/1.1709079 (1967).
53. Boyd, G. D., Buehler, E. & Storz, F. G. Linear and nonlinear optical properties of $ZnGeP_2$ and CdSe. *Applied Physics Letters* **18**, 301–304, https://doi.org/10.1063/1.1653673 (1971).
54. Boyd, G., Kasper, H. & McFee, J. Linear and nonlinear optical properties of $AgGaS_2$, $CuGaS_2$, and $CuInS_2$, and theory of the wedge technique for the measurement of nonlinear coefficients. *IEEE Journal of Quantum Electronics* **7**, 563–573, https://doi.org/10.1109/jqe.1971.1076588 (1971).
55. Boyd, G., Buehler, E., Storz, F. & Wernick, J. Linear and nonlinear optical properties of ternary $A^{II}B^{IV}C_2^{V}$ chalcopyrite semiconductors. *IEEE Journal of Quantum Electronics* **8**, 419–426, https://doi.org/10.1109/jqe.1972.1076982 (1972).
56. Boyd, G., Kasper, H., McFee, J. & Storz, F. Linear and nonlinear optical properties of some ternary selenides. *IEEE Journal of Quantum Electronics* **8**, 900–908, https://doi.org/10.1109/jqe.1972.1076900 (1972).
57. Brannon, J. H., Lankard, J. R., Baise, A. I., Burns, F. & Kaufman, J. Excimer laser etching of polyimide. *Journal of Applied Physics* **58**, 2036–2043, https://doi.org/10.1063/1.336012 (1985).
58. Brasse, Y. *et al*. Magnetic and electric resonances in particle-to-film-coupled functional nanostructures. *ACS Applied Materials & Interfaces* **10**, 3133–3141, https://doi.org/10.1021/acsami.7b16941 (2018).
59. Bright, T., Watjen, J., Zhang, Z., Muratore, C. & Voevodin, A. Optical properties of HfO_2 thin films deposited by magnetron sputtering: From the visible to the far-infrared. *Thin Solid Films* **520**, 6793–6802, https://doi.org/10.1016/j.tsf.2012.07.037 (2012).
60. Bright, T. J. *et al*. Infrared optical properties of amorphous and nanocrystalline Ta_2O_5 thin films. *Journal of Applied Physics* **114**, https://doi.org/10.1063/1.4819325 (2013).

61. Brimhall, N. *et al*. Measured optical constants of copper from 10 nm to 35 nm. *Optics Express* **17**, 23873, https://doi.org/10.1364/oe.17.023873 (2009).
62. Bristow, A. D., Rotenberg, N. & van Driel, H. M. Two-photon absorption and kerr coefficients of silicon for 850–2200nm. *Applied Physics Letters* **90**, https://doi.org/10.1063/1.2737359 (2007).
63. Bucciarelli, A. *et al*. A comparative study of the refractive index of silk protein thin films towards biomaterial based optical devices. *Optical Materials* **78**, 407–414, https://doi.org/10.1016/j.optmat.2018.02.058 (2018).
64. Burnett, J. H., Kaplan, S. G., Stover, E. & Phenis, A. Refractive index measurements of Ge. In LeVan, P. D., Sood, A. K., Wijewarnasuriya, P. & D'Souza, A. I. (eds.) *Infrared Sensors, Devices, and Applications VI*, https://doi.org/10.1117/12.2237978 (SPIE, 2016).
65. Caldwell, R. S. & Fan, H. Y. Optical properties of tellurium and selenium. *Physical Review* **114**, 664–675, https://doi.org/10.1103/physrev.114.664 (1959).
66. Callcott, T. A. & Arakawa, E. T. Ultraviolet optical properties of Li. *Journal of the Optical Society of America* **64**, 839, https://doi.org/10.1364/josa.64.000839 (1974).
67. Carvajal, J. J. *et al*. Structural and optical properties of RbTiOPO4:Nb crystals. *Journal of Physics: Condensed Matter* **19**, 116214, https://doi.org/10.1088/0953-8984/19/11/116214 (2007).
68. Chandler-Horowitz, D. & Amirtharaj, P. M. High-accuracy, midinfrared ($450\ cm^{-1} \leq \omega \leq 4000\ cm^{-1}$) refractive index values of silicon. *Journal of Applied Physics* **97**, https://doi.org/10.1063/1.1923612 (2005).
69. Chemnitz, M. *et al*. Hybrid soliton dynamics in liquid-core fibres. *Nature Communications* **8**, https://doi.org/10.1038/s41467-017-00033-5 (2017).
70. Chen, L. & Lynch, D. W. The optical properties of $AuAl_2$ and $PtAl_2$. *physica status solidi (b)* **148**, 387–394, https://doi.org/10.1002/pssb.2221480136 (1988).
71. Chen, C. *et al*. New nonlinear-optical crystal: LiB_3O_5. *Journal of the Optical Society of America B* **6**, 616, https://doi.org/10.1364/josab.6.000616 (1989).
72. Chen, C.-W. *et al*. Optical properties of organometal halide perovskite thin films and general device structure design rules for perovskite single and tandem solar cells. *Journal of Materials Chemistry A* **3**, 9152–9159, https://doi.org/10.1039/c4ta05237d (2015).
73. Cheng, F. *et al*. Epitaxial growth of atomically smooth aluminum on silicon and its intrinsic optical properties. *ACS Nano* **10**, 9852–9860, https://doi.org/10.1021/acsnano.6b05556 (2016).
74. Chengchao, W., Xingcan, L., Jianyu, T. & Linhua, L. Experimental measurement of optical constant of biodiesel by double optical pathlength transmission method. *Laser & Optoelectronics Progress* **52**, 051206, https://doi.org/10.3788/lop52.051206 (2015).
75. Choy, M. M. & Byer, R. L. Accurate second-order susceptibility measurements of visible and infrared nonlinear crystals. *Physical Review B* **14**, 1693–1706, https://doi.org/10.1103/physrevb.14.1693 (1976).
76. Ciddor, P. E. Refractive index of air: new equations for the visible and near infrared. *Applied Optics* **35**, 1566, https://doi.org/10.1364/ao.35.001566 (1996).
77. Ciesielski, A., Skowronski, L., Trzcinski, M. & Szoplik, T. Controlling the optical parameters of self-assembled silver films with wetting layers and annealing. *Applied Surface Science* **421**, 349–356, https://doi.org/10.1016/j.apsusc.2017.01.039 (2017).
78. Ciesielski, A., Skowronski, L., Pacuski, W. & Szoplik, T. Permittivity of ge, te and se thin films in the 200–1500 nm spectral range. predicting the segregation effects in silver. *Materials Science in Semiconductor Processing* **81**, 64–67, https://doi.org/10.1016/j.mssp.2018.03.003 (2018).
79. Ciesielski, A. *et al*. Evidence of germanium segregation in gold thin films. *Surface Science* **674**, 73–78, https://doi.org/10.1016/j.susc.2018.03.020 (2018).
80. Connolly, J., diBenedetto, B. & Donadio, R. Specifications of raytran material. In Fischer, R. E. (ed.) *Contemporary Optical Systems and Components Specifications*, https://doi.org/10.1117/12.957359 (SPIE, 1979).
81. Coulter, J. K., Hass, G. & Ramsey, J. B. Optical constants and reflectance and transmittance of evaporated rhodium films in the visible. *Journal of the Optical Society of America* **63**, 1149, https://doi.org/10.1364/josa.63.001149 (1973).
82. Cunningham, P. D. *et al*. Broadband terahertz characterization of the refractive index and absorption of some important polymeric and organic electro-optic materials. *Journal of Applied Physics* **109**, 043505–043505–5, https://doi.org/10.1063/1.3549120 (2011).
83. Cuthbertson, C. & Cuthbertson, M. On the refraction and dispersion of neon. *Proceedings of the Royal Society of London. Series A, Containing Papers of a Mathematical and Physical Character* **83**, 149–151, https://doi.org/10.1098/rspa.1910.0001 (1910).
84. Cuthbertson, C. & Cuthbertson, M. The refraction and dispersion of argon, and redeterminations of the dispersion of helium, neon, krypton, and xenon. *Proceedings of the Royal Society of London. Series A, Containing Papers of a Mathematical and Physical Character* **84**, 13–15, https://doi.org/10.1098/rspa.1910.0052 (1910).
85. Cuthbertson, C. & Cuthbertson, M. On the refraction and dispersion of the halogens, halogen acids, ozone, steam, oxides of nitrogen and ammonia. *Philosophical Transactions of the Royal Society of London. Series A, Containing Papers of a Mathematical or Physical Character* **213**, 1–26, https://doi.org/10.1098/rsta.1914.0001 (1914).
86. Cuthbertson, C. & Cuthbertson, M. The refraction and dispersion of neon and helium. *Proceedings of the Royal Society of London. Series A, Containing Papers of a Mathematical and Physical Character* **135**, 40–47, https://doi.org/10.1098/rspa.1932.0019 (1932).
87. Daimon, M. & Masumura, A. High-accuracy measurements of the refractive index and its temperature coefficient of calcium fluoride in a wide wavelength range from 138 to 2326 nm. *Applied Optics* **41**, 5275, https://doi.org/10.1364/ao.41.005275 (2002).
88. Daimon, M. & Masumura, A. Measurement of the refractive index of distilled water from the near-infrared region to the ultraviolet region. *Applied Optics* **46**, 3811, https://doi.org/10.1364/ao.46.003811 (2007).
89. Dalzell, W. H. & Sarofim, A. F. Optical constants of soot and their application to heat-flux calculations. *Journal of Heat Transfer* **91**, 100–104, https://doi.org/10.1115/1.3580063 (1969).
90. Das, S., Bhar, G. C., Gangopadhyay, S. & Ghosh, C. Linear and nonlinear optical properties of $ZnGeP_2$ crystal for infrared laser device applications: revisited. *Applied Optics* **42**, 4335, https://doi.org/10.1364/ao.42.004335 (2003).
91. David, M. *et al*. Structure and mid-infrared optical properties of spin-coated polyethylene films developed for integrated photonics applications. *Optical Materials Express* **12**, 2168, https://doi.org/10.1364/ome.458667 (2022).
92. DeBell, A. G. *et al*. Cryogenic refractive indices and temperature coefficients of cadmium telluride from 6 μm to 22 μm. *Applied Optics* **18**, 3114, https://doi.org/10.1364/ao.18.003114 (1979).
93. DeSalvo, R., Said, A., Hagan, D., Van Stryland, E. & Sheik-Bahae, M. Infrared to ultraviolet measurements of two-photon absorption and n_2 in wide bandgap solids. *IEEE Journal of Quantum Electronics* **32**, 1324–1333, https://doi.org/10.1109/3.511545 (1996).
94. DeVore, J. R. Refractive indices of rutile and sphalerite. *Journal of the Optical Society of America* **41**, 416, https://doi.org/10.1364/josa.41.000416 (1951).
95. Debenham, M. Refractive indices of zinc sulfide in the 0.405–13-μm wavelength range. *Applied Optics* **23**, 2238, https://doi.org/10.1364/ao.23.002238 (1984).
96. Djurišić, A. B. & Li, E. H. Optical properties of graphite. *Journal of Applied Physics* **85**, 7404–7410, https://doi.org/10.1063/1.369370 (1999).
97. Djurišić, A., Li, E., Rakić, D. & Majewski, M. Modeling the optical properties of AlSb, GaSb, and InSb. *Applied Physics A: Materials Science & Processing* **70**, 29–32, https://doi.org/10.1007/s003390050006 (2000).
98. Dodge, M. J. Refractive properties of magnesium fluoride. *Applied Optics* **23**, 1980, https://doi.org/10.1364/ao.23.001980 (1984).

99. Dore, P. *et al*. Infrared properties of chemical-vapor deposition polycrystalline diamond windows. *Applied Optics* **37**, 5731, https://doi.org/10.1364/ao.37.005731 (1998).
100. Edwards, D. F. & Ochoa, E. Infrared refractive index of silicon. *Applied Optics* **19**, 4130, https://doi.org/10.1364/ao.19.004130 (1980).
101. Eimerl, D., Davis, L., Velsko, S., Graham, E. K. & Zalkin, A. Optical, mechanical, and thermal properties of barium borate. *Journal of Applied Physics* **62**, 1968–1983, https://doi.org/10.1063/1.339536 (1987).
102. El-Kashef, H. The necessary requirements imposed on polar dielectric laser dye solvents. *Physica B: Condensed Matter* **279**, 295–301, https://doi.org/10.1016/s0921-4526(99)00856-x (2000).
103. Ensley, T. R. & Bambha, N. K. Ultrafast nonlinear refraction measurements of infrared transmitting materials in the mid-wave infrared. *Optics Express* **27**, 37940, https://doi.org/10.1364/oe.380702 (2019).
104. Ermolaev, G. A., Yakubovsky, D. I., Stebunov, Y. V., Arsenin, A. V. & Volkov, V. S. Spectral ellipsometry of monolayer transition metal dichalcogenides: Analysis of excitonic peaks in dispersion. *Journal of Vacuum Science & Technology B, Nanotechnology and Microelectronics: Materials, Processing, Measurement, and Phenomena* **38**, https://doi.org/10.1116/1.5122683 (2019).
105. Ermolaev, G. A. *et al*. Broadband optical properties of monolayer and bulk MoS_2. *npj 2D Materials and Applications* **4**, https://doi.org/10.1038/s41699-020-0155-x (2020).
106. Ermolaev, G. A. *et al*. Express determination of thickness and dielectric function of single-walled carbon nanotube films. *Applied Physics Letters* **116**, https://doi.org/10.1063/5.0012933 (2020).
107. Ermolaev, G. A. *et al*. Broadband optical properties of atomically thin PtS_2 and $PtSe_2$. *Nanomaterials* **11**, 3269, https://doi.org/10.3390/nano11123269 (2021).
108. Ermolaev, G. A. *et al*. Broadband optical constants and nonlinear properties of SnS_2 and $SnSe_2$. *Nanomaterials* **12**, 141, https://doi.org/10.3390/nano12010141 (2021).
109. Ermolaev, G. A. *et al*. Giant optical anisotropy in transition metal dichalcogenides for next-generation photonics. *Nature Communications* **12**, https://doi.org/10.1038/s41467-021-21139-x (2021).
110. Ermolaev, G. A. *et al*. Spectroscopic ellipsometry of large area monolayer WS_2 and WSe_2 films. In *AIP Conference Proceedings*, https://doi.org/10.1063/5.0054947 (AIP Publishing, 2021).
111. Ermolaev, G. *et al*. Topological phase singularities in atomically thin high-refractive-index materials. *Nature Communications* **13**, https://doi.org/10.1038/s41467-022-29716-4 (2022).
112. Ermolaev, G. *et al*. Giant and tunable excitonic optical anisotropy in single-crystal halide perovskites. *Nano Letters* **23**, 2570–2577, https://doi.org/10.1021/acs.nanolett.2c04792 (2023).
113. Ermolaev, G. A. *et al*. Anisotropic optical properties of monolayer aligned single-walled carbon nanotubes. *physica status solidi (RRL) – Rapid Research Letters* 2300199, https://doi.org/10.1002/pssr.202300199 (2023).
114. Ermolov, A., Mak, K. F., Frosz, M. H., Travers, J. C. & Russell, P. S. J. Supercontinuum generation in the vacuum ultraviolet through dispersive-wave and soliton-plasma interaction in a noble-gas-filled hollow-core photonic crystal fiber. *Physical Review A* **92**, https://doi.org/10.1103/physreva.92.033821 (2015).
115. Ewbank, M. D. *et al*. The temperature dependence of optical and mechanical properties of Tl_3AsSe_3. *Journal of Applied Physics* **51**, 3848–3852, https://doi.org/10.1063/1.328128 (1980).
116. Fang, S., Liu, H., Huang, L. & Ye, N. Growth and optical properties of nonlinear $LuAl_3(BO_3)_4$ crystals. *Optics Express* **21**, 16415, https://doi.org/10.1364/oe.21.016415 (2013).
117. Fang, M. *et al*. Layer-dependent dielectric permittivity of topological insulator Bi_2Se_3 thin films. *Applied Surface Science* **509**, 144822, https://doi.org/10.1016/j.apsusc.2019.144822 (2020).
118. Feldman, A. & Horowitz, D. Refractive index of cuprous chloride*. *Journal of the Optical Society of America* **59**, 1406, https://doi.org/10.1364/josa.59.001406 (1969).
119. Fern, R. E. & Onton, A. Refractive index of AlAs. *Journal of Applied Physics* **42**, 3499–3500, https://doi.org/10.1063/1.1660760 (1971).
120. Fernández-Perea, M. *et al*. Determination of optical constants of scandium films in the 20–1000 eV range. *Journal of the Optical Society of America A* **23**, 2880, https://doi.org/10.1364/josaa.23.002880 (2006).
121. Fernández-Perea, M. *et al*. Optical constants of electron-beam evaporated boron films in the 6.8–900 eV photon energy range. *Journal of the Optical Society of America A* **24**, 3800, https://doi.org/10.1364/josaa.24.003800 (2007).
122. Fernández-Perea, M. *et al*. Optical constants of Yb films in the 23–1700 eV range. *Journal of the Optical Society of America A* **24**, 3691, https://doi.org/10.1364/josaa.24.003691 (2007).
123. Fernández-Perea, M. *et al*. Transmittance and optical constants of Pr films in the 4–1600ev spectral range. *Journal of Applied Physics* **103**, https://doi.org/10.1063/1.2939269 (2008).
124. Fernández-Perea, M. *et al*. Transmittance and optical constants of Eu films from 8.3 to 1400 eV. *Journal of Applied Physics* **104**, https://doi.org/10.1063/1.2982391 (2008).
125. Fernández-Perea, M. *et al*. Transmittance and optical constants of Ce films in the 6–1200ev spectral range. *Journal of Applied Physics* **103**, https://doi.org/10.1063/1.2901137 (2008).
126. Fernández-Perea, M. *et al*. Optical constants of evaporation-deposited silicon monoxide films in the 7.1–800 eV photon energy range. *Journal of Applied Physics* **105**, https://doi.org/10.1063/1.3123768 (2009).
127. Fernández-Perea, M. *et al*. Transmittance and optical constants of Ho films in the 3–1340 eV spectral range. *Journal of Applied Physics* **109**, https://doi.org/10.1063/1.3556451 (2011).
128. Ferrera, M., Magnozzi, M., Bisio, F. & Canepa, M. Temperature-dependent permittivity of silver and implications for thermoplasmonics. *Physical Review Materials* **3**, https://doi.org/10.1103/physrevmaterials.3.105201 (2019).
129. Ferrini, R., Patrini, M. & Franchi, S. Optical functions from 0.02 to 6 eV of $Al_xGa_{1-x}Sb$/GaSb epitaxial layers. *Journal of Applied Physics* **84**, 4517–4524, https://doi.org/10.1063/1.368677 (1998).
130. Fischer, M. P. *et al*. Coherent field transients below 15 THz from phase-matched difference frequency generation in 4H-SiC. *Optics Letters* **42**, 2687, https://doi.org/10.1364/ol.42.002687 (2017).
131. Fleming, J. W. Dispersion in GeO_2-SiO_2 glasses. *Applied Optics* **23**, 4486, https://doi.org/10.1364/ao.23.004486 (1984).
132. Flom, S. R., Beadie, G., Bayya, S. S., Shaw, B. & Auxier, J. M. Ultrafast z-scan measurements of nonlinear optical constants of window materials at 772, 1030, and 1550 nm. *Applied Optics* **54**, F123, https://doi.org/10.1364/ao.54.00f123 (2015).
133. Franta, D., Nečas, D. & Ohlídal, I. Universal dispersion model for characterization of optical thin films over a wide spectral range: application to hafnia. *Applied Optics* **54**, 9108, https://doi.org/10.1364/ao.54.009108 (2015).
134. French, R. H. *et al*. Optical properties of materials for concentrator photovoltaic systems. In *2009 34th IEEE Photovoltaic Specialists Conference (PVSC)*, https://doi.org/10.1109/pvsc.2009.5411657 (IEEE, 2009).
135. Frisenda, R. *et al*. Characterization of highly crystalline lead iodide nanosheets prepared by room-temperature solution processing. *Nanotechnology* **28**, 455703, https://doi.org/10.1088/1361-6528/aa8e5c (2017).
136. Fujii, Y. & Sakudo, T. Dielectric and optical properties of $KTaO_3$. *Journal of the Physical Society of Japan* **41**, 888–893, https://doi.org/10.1143/jpsj.41.888 (1976).
137. Gan, F. Optical properties of fluoride glasses: a review. *Journal of Non-Crystalline Solids* **184**, 9–20, https://doi.org/10.1016/0022-3093(94)00592-3 (1995).
138. Gant, P. *et al*. Optical contrast and refractive index of natural van der waals heterostructure nanosheets of franckeite. *Beilstein Journal of Nanotechnology* **8**, 2357–2362, https://doi.org/10.3762/bjnano.8.235 (2017).

139. Gao, L., Lemarchand, F. & Lequime, M. Comparison of different dispersion models for single layer optical thin film index determination. *Thin Solid Films* **520**, 501–509, https://doi.org/10.1016/j.tsf.2011.07.028 (2011).
140. Gao, L., Lemarchand, F. & Lequime, M. Exploitation of multiple incidences spectrometric measurements for thin film reverse engineering. *Optics Express* **20**, 15734, https://doi.org/10.1364/oe.20.015734 (2012).
141. Gao, L., Lemarchand, F. & Lequime, M. Refractive index determination of SiO_2 layer in the UV/Vis/NIR range: spectrophotometric reverse engineering on single and bi-layer designs. *Journal of the European Optical Society: Rapid Publications* **8**, https://doi.org/10.2971/jeos.2013.13010 (2013).
142. García-Cortés, S. *et al*. Transmittance and optical constants of Lu films in the 3–1800 eV spectral range. *Journal of Applied Physics* **108**, https://doi.org/10.1063/1.3481062 (2010).
143. Geints, Y. E. *et al*. Kerr-driven nonlinear refractive index of air at 800 and 400 nm measured through femtosecond laser pulse filamentation. *Applied Physics Letters* **99**, https://doi.org/10.1063/1.3657774 (2011).
144. Ghosal, S., Ebert, J. L. & Self, S. A. The infrared refractive indices of $CHBr_3$, CCl_4 and CS_2. *Infrared Physics* **34**, 621–628, https://doi.org/10.1016/0020-0891(93)90120-v (1993).
145. Ghosh, G. Dispersion-equation coefficients for the refractive index and birefringence of calcite and quartz crystals. *Optics Communications* **163**, 95–102, https://doi.org/10.1016/s0030-4018(99)00091-7 (1999).
146. Giannios, P. *et al*. Complex refractive index of normal and malignant human colorectal tissue in the visible and near-infrared. *Journal of Biophotonics* **10**, 303–310, https://doi.org/10.1002/jbio.201600001 (2016).
147. Giannios, P. *et al*. Visible to near-infrared refractive properties of freshly-excised human-liver tissues: marking hepatic malignancies. *Scientific Reports* **6**, https://doi.org/10.1038/srep27910 (2016).
148. Gomez, M. S., Guerra, J. M. & Vilches, F. Weighted nonlinear regression analysis of a Sellmeier expansion: comparison of several nonlinear fits of CdS dispersion. *Applied Optics* **24**, 1147, https://doi.org/10.1364/ao.24.001147 (1985).
149. Grace, E., Butcher, A., Monroe, J. & Nikkel, J. A. Index of refraction, Rayleigh scattering length, and Sellmeier coefficients in solid and liquid argon and xenon. *Nuclear Instruments and Methods in Physics Research Section A: Accelerators, Spectrometers, Detectors and Associated Equipment* **867**, 204–208, https://doi.org/10.1016/j.nima.2017.06.031 (2017).
150. Green, M. A. & Keevers, M. J. Optical properties of intrinsic silicon at 300 K. *Progress in Photovoltaics: Research and Applications* **3**, 189–192, https://doi.org/10.1002/pip.4670030303 (1995).
151. Green, M. A. Self-consistent optical parameters of intrinsic silicon at 300 K including temperature coefficients. *Solar Energy Materials and Solar Cells* **92**, 1305–1310, https://doi.org/10.1016/j.solmat.2008.06.009 (2008).
152. Griesmann, U. & Burnett, J. H. Refractivity of nitrogen gas in the vacuum ultraviolet. *Optics Letters* **24**, 1699, https://doi.org/10.1364/ol.24.001699 (1999).
153. Grudinin, D. V. *et al*. Hexagonal boron nitride nanophotonics: a record-breaking material for the ultraviolet and visible spectral ranges. *Materials Horizons* **10**, 2427–2435, https://doi.org/10.1039/d3mh00215b (2023).
154. Gu, H. *et al*. Layer-dependent dielectric and optical properties of centimeter-scale 2D WSe_2: evolution from a single layer to few layers. *Nanoscale* **11**, 22762–22771, https://doi.org/10.1039/c9nr04270a (2019).
155. Guo, Z. *et al*. Complete dielectric tensor and giant optical anisotropy in quasi-one-dimensional $ZrTe_5$. *ACS Materials Letters* **3**, 525–534, https://doi.org/10.1021/acsmaterialslett.1c00026 (2021).
156. Guo, Z., Gu, H., Fang, M., Ye, L. & Liu, S. Giant in-plane optical and electronic anisotropy of tellurene: a quantitative exploration. *Nanoscale* **14**, 12238–12246, https://doi.org/10.1039/d2nr03226k (2022).
157. Guo, Z., Gu, H., Yu, Y., Wei, Z. & Liu, S. Broadband and incident-angle-modulation near-infrared polarizers based on optically anisotropic SnSe. *Nanomaterials* **13**, 134, https://doi.org/10.3390/nano13010134 (2022).
158. Gupta, V. *et al*. Mechanotunable surface lattice resonances in the visible optical range by soft lithography templates and directed self-assembly. *ACS Applied Materials & Interfaces* **11**, 28189–28196, https://doi.org/10.1021/acsami.9b08871 (2019).
159. Gupta, V. *et al*. Advanced colloidal sensors enabled by an out-of-plane lattice resonance. *Advanced Photonics Research* **3**, https://doi.org/10.1002/adpr.202200152 (2022).
160. Hagemann, H.-J., Gudat, W. & Kunz, C. Optical constants from the far infrared to the x-ray region: Mg, Al, Cu, Ag, Au, Bi, C, and Al_2O_3. *Journal of the Optical Society of America* **65**, 742, https://doi.org/10.1364/josa.65.000742 (1975).
161. Hale, G. M. & Querry, M. R. Optical constants of water in the 200-nm to 200-μm wavelength region. *Applied Optics* **12**, 555, https://doi.org/10.1364/ao.12.000555 (1973).
162. Hanson, F. & Dick, D. Blue parametric generation from temperature-tuned LiB_3O_5. *Optics Letters* **16**, 205, https://doi.org/10.1364/ol.16.000205 (1991).
163. Hartnett, T., Bernstein, S., Maguire, E. & Tustison, R. Optical properties of ALON (aluminum oxynitride). *Infrared Physics & Technology* **39**, 203–211, https://doi.org/10.1016/s1350-4495(98)00007-3 (1998).
164. Hass, G. & Salzberg, C. D. Optical properties of silicon monoxide in the wavelength region from 0.24 to 14.0 microns. *Journal of the Optical Society of America* **44**, 181, https://doi.org/10.1364/josa.44.000181 (1954).
165. Hass, G., Jacobus, G. F. & Hunter, W. R. Optical properties of evaporated iridium in the vacuum ultraviolet from 500 Å to 2000 Å. *Journal of the Optical Society of America* **57**, 758, https://doi.org/10.1364/josa.57.000758 (1967).
166. Heitmann, W. & Ritter, E. Production and properties of vacuum evaporated films of thorium fluoride. *Applied Optics* **7**, 307, https://doi.org/10.1364/ao.7.000307 (1968).
167. Herguedas, N. & Carretero, E. Optical properties in mid-infrared range of silicon oxide thin films with different stoichiometries. *Nanomaterials* **13**, 2749, https://doi.org/10.3390/nano13202749 (2023).
168. Horcholle, B. *et al*. Growth and study of Tb^{3+} doped Nb_2O_5 thin films by radiofrequency magnetron sputtering: Photoluminescence properties. *Applied Surface Science* **597**, 153711, https://doi.org/10.1016/j.apsusc.2022.153711 (2022).
169. Hrabovský, J., Kučera, M., Paloušová, L., Bi, L. & Veis, M. Optical characterization of $Y_3Al_5O_{12}$ and $Lu_3Al_5O_{12}$ single crystals. *Optical Materials Express* **11**, 1218, https://doi.org/10.1364/ome.417670 (2021).
170. Hsu, C. *et al*. Thickness-dependent refractive index of 1L, 2L, and 3L MoS_2, $MoSe_2$, WS_2, and WSe_2. *Advanced Optical Materials* **7**, https://doi.org/10.1002/adom.201900239 (2019).
171. Hulme, K. F., Jones, O., Davies, P. H. & Hobden, M. V. Synthetic proustite (Ag_3AsS_3): A new crystal for optical mixing. *Applied Physics Letters* **10**, 133–135, https://doi.org/10.1063/1.1754880 (1967).
172. Hurlbut, W. C., Lee, Y.-S., Vodopyanov, K. L., Kuo, P. S. & Fejer, M. M. Multiphoton absorption and nonlinear refraction of GaAs in the mid-infrared. *Optics Letters* **32**, 668, https://doi.org/10.1364/ol.32.000668 (2007).
173. Iezzi, B. *et al*. Electrohydrodynamic jet printing of 1D photonic crystals: Part II–optical design and reflectance characteristics. *Advanced Materials Technologies* **5**, https://doi.org/10.1002/admt.202000431 (2020).
174. Inagaki, T., Hamm, R. N., Arakawa, E. T. & Painter, L. R. Optical and dielectric properties of DNA in the extreme ultraviolet. *The Journal of Chemical Physics* **61**, 4246–4250, https://doi.org/10.1063/1.1681724 (1974).
175. Inagaki, T., Arakawa, E. T., Birkhoff, R. D. & Williams, M. W. Optical properties of liquid Na between 0.6 and 3.8 eV. *Physical Review B* **13**, 5610–5612, https://doi.org/10.1103/physrevb.13.5610 (1976).
176. Inagaki, T., Emerson, L. C., Arakawa, E. T. & Williams, M. W. Optical properties of solid Na and Li between 0.6 and 3.8 eV. *Physical Review B* **13**, 2305–2313, https://doi.org/10.1103/physrevb.13.2305 (1976).
177. Inagaki, T., Arakawa, E. T. & Williams, M. W. Optical properties of liquid mercury. *Physical Review B* **23**, 5246–5262, https://doi.org/10.1103/physrevb.23.5246 (1981).

178. Ishteev, A. *et al*. Investigation of structural and optical properties of $MAPbBr_3$ monocrystals under fast electron irradiation. *Journal of Materials Chemistry C* **10**, 5821–5828, https://doi.org/10.1039/d2tc00128d (2022).
179. Islam, K. M. *et al*. In-plane and out-of-plane optical properties of monolayer, few-layer, and thin-film MoS_2 from 190 to 1700 nm and their application in photonic device design. *Advanced Photonics Research* **2**, https://doi.org/10.1002/adpr.202000180 (2021).
180. Ives, H. E. & Briggs, H. B. The optical constants of potassium. *Journal of the Optical Society of America* **26**, 238, https://doi.org/10.1364/josa.26.000238 (1936).
181. Ives, H. E. & Briggs, H. B. Optical constants of rubidium and cesium. *Journal of the Optical Society of America* **27**, 395, https://doi.org/10.1364/josa.27.000395 (1937).
182. Ives, H. E. & Briggs, H. B. The optical constants of sodium. *Journal of the Optical Society of America* **27**, 181, https://doi.org/10.1364/josa.27.000181 (1937).
183. Jansonas, G., Budriūnas, R., Vengris, M. & Varanavičius, A. Interferometric measurements of nonlinear refractive index in the infrared spectral range. *Optics Express* **30**, 30507, https://doi.org/10.1364/oe.458850 (2022).
184. Jöbsis, H. J. *et al*. Recombination and localization: Unfolding the pathways behind conductivity losses in $Cs_2AgBiBr_6$ thin films. *Applied Physics Letters* **119**, https://doi.org/10.1063/5.0061899 (2021).
185. Jellison, G. Optical functions of silicon determined by two-channel polarization modulation ellipsometry. *Optical Materials* **1**, 41–47, https://doi.org/10.1016/0925-3467(92)90015-f (1992).
186. Jellison, G. Optical functions of GaAs, GaP, and Ge determined by two-channel polarization modulation ellipsometry. *Optical Materials* **1**, 151–160, https://doi.org/10.1016/0925-3467(92)90022-f (1992).
187. Jellison, G., Haynes, T. & Burke, H. Optical functions of silicon-germanium alloys determined using spectroscopic ellipsometry. *Optical Materials* **2**, 105–117, https://doi.org/10.1016/0925-3467(93)90035-y (1993).
188. Jellison, G. E. *et al*. Refractive index of sodium iodide. *Journal of Applied Physics* **111**, https://doi.org/10.1063/1.3689746 (2012).
189. Jiang, Y., Pillai, S. & Green, M. A. Realistic silver optical constants for plasmonics. *Scientific Reports* **6**, https://doi.org/10.1038/srep30605 (2016).
190. Johnson, P. B. & Christy, R. W. Optical constants of the noble metals. *Physical Review B* **6**, 4370–4379, https://doi.org/10.1103/physrevb.6.4370 (1972).
191. Johnson, P. & Christy, R. Optical constants of transition metals: Ti, V, Cr, Mn, Fe, Co, Ni, and Pd. *Physical Review B* **9**, 5056–5070, https://doi.org/10.1103/physrevb.9.5056 (1974).
192. Joseph, S., Sarkar, S. & Joseph, J. Grating-coupled surface plasmon-polariton sensing at a flat metal–analyte interface in a hybrid-configuration. *ACS Applied Materials & Interfaces* **12**, 46519–46529, https://doi.org/10.1021/acsami.0c12525 (2020).
193. Joseph, S., Sarkar, S., Khan, S. & Joseph, J. Exploring the optical bound state in the continuum in a dielectric grating coupled plasmonic hybrid system. *Advanced Optical Materials* **9**, https://doi.org/10.1002/adom.202001895 (2021).
194. Jung, G.-H., Yoo, S. & Park, Q.-H. Measuring the optical permittivity of two-dimensional materials without a priori knowledge of electronic transitions. *Nanophotonics* **8**, 263–270, https://doi.org/10.1515/nanoph-2018-0120 (2018).
195. Křen, P. Comment on "Precision refractive index measurements of air, N_2, O_2, Ar, and CO_2 with a frequency comb". *Applied Optics* **50**, 6484, https://doi.org/10.1364/ao.50.006484 (2011).
196. König, T. A. F. *et al*. Electrically tunable plasmonic behavior of nanocube–polymer nanomaterials induced by a redox-active electrochromic polymer. *ACS Nano* **8**, 6182–6192, https://doi.org/10.1021/nn501601e (2014).
197. Kabaciński, P., Kardaś, T. M., Stepanenko, Y. & Radzewicz, C. Nonlinear refractive index measurement by SPM-induced phase regression. *Optics Express* **27**, 11018, https://doi.org/10.1364/oe.27.011018 (2019).
198. Kabelka, V. I., Piskarskas, A. S., Stabinis, A. Y. & Sher, R. L. Group matching of interacting light pulses in nonlinear crystals. *Soviet Journal of Quantum Electronics* **5**, 255–256, https://doi.org/10.1070/qe1975v005n02abeh010943 (1975).
199. Kachare, A. H., Spitzer, W. G. & Fredrickson, J. E. Refractive index of ion-implanted GaAs. *Journal of Applied Physics* **47**, 4209–4212, https://doi.org/10.1063/1.323292 (1976).
200. Kaiser, W., Spitzer, W. G., Kaiser, R. H. & Howarth, L. E. Infrared properties of CaF_2, SrF_2, and BaF_2. *Physical Review* **127**, 1950–1954, https://doi.org/10.1103/physrev.127.1950 (1962).
201. Kaminskii, A. A. *et al*. Mechanical and optical properties of Lu_2O_3 host-ceramics for Ln^{3+} lasants. *Laser Physics Letters* **5**, 300–303, https://doi.org/10.1002/lapl.200710128 (2007).
202. Kato, K. High-power difference-frequency generation at 4.4–5.7 μm in $LiIO_3$. *IEEE Journal of Quantum Electronics* **21**, 119–120, https://doi.org/10.1109/jqe.1985.1072617 (1985).
203. Kato, K. & Takaoka, E. Sellmeier and thermo-optic dispersion formulas for KTP. *Applied Optics* **41**, 5040, https://doi.org/10.1364/ao.41.005040 (2002).
204. Kato, K. & Umemura, N. Sellmeier equations for GaS and GaSe and their applications to the nonlinear optics in GaS_xSe_{1-x}. *Optics Letters* **36**, 746, https://doi.org/10.1364/ol.36.000746 (2011).
205. Kato, K., Tanno, F. & Umemura, N. Sellmeier and thermo-optic dispersion formulas for GaSe (revisited). *Applied Optics* **52**, 2325, https://doi.org/10.1364/ao.52.002325 (2013).
206. Kato, K., Petrov, V. & Umemura, N. Phase-matching properties of yellow color $HgGa_2S_4$ for shg and sfg in the 0.944–10.5910 μm range. *Applied Optics* **55**, 3145, https://doi.org/10.1364/ao.55.003145 (2016).
207. Kato, K., Umemura, N. & Petrov, V. Sellmeier and thermo-optic dispersion formulas for $CdGa_2S_4$ and their application to the nonlinear optics of $Hg_{1-x}Cd_xGa_2S_4$. *Optics Communications* **386**, 49–52, https://doi.org/10.1016/j.optcom.2016.10.054 (2017).
208. Kato, K. *et al*. Phase-matching properties of $LiGaS_2$ in the 1.025–10.5910 μm spectral range. *Optics Letters* **42**, 4363, https://doi.org/10.1364/ol.42.004363 (2017).
209. Kato, K., Miyata, K., Badikov, V. V. & Petrov, V. Phase-matching properties of $BaGa_2GeSe_6$ for three-wave interactions in the 0.778–10.5910 μm spectral range. *Applied Optics* **57**, 7440, https://doi.org/10.1364/ao.57.007440 (2018).
210. Kato, K., Badikov, V. V., Miyata, K. & Petrov, V. Refined Sellmeier equations for $BaGa_4S_7$. *Applied Optics* **60**, 6600, https://doi.org/10.1364/ao.430424 (2021).
211. Kato, K., Miyata, K. & Petrov, V. Refined Sellmeier equations for $AgGaSe_2$ up to 18 μm. *Applied Optics* **60**, 805, https://doi.org/10.1364/ao.401828 (2021).
212. Kato, K., Banerjee, S. & Umemura, N. Phase-matching properties of $AgGa_{0.86}In_{0.14}S_2$ for three-wave interactions in the 0.615–10.5910 μm spectral range. *Optical Materials Express* **11**, 2800, https://doi.org/10.1364/ome.428688 (2021).
213. Kawashima, T., Yoshikawa, H., Adachi, S., Fuke, S. & Ohtsuka, K. Optical properties of hexagonal GaN. *Journal of Applied Physics* **82**, 3528–3535, https://doi.org/10.1063/1.365671 (1997).
214. Kawka, P. A. & Buckius, R. O. Optical properties of polyimide films in the infrared. *International Journal of Thermophysics* **22**, 517–534, https://doi.org/10.1023/a:1010797620483 (2001).
215. Kedenburg, S., Vieweg, M., Gissibl, T. & Giessen, H. Linear refractive index and absorption measurements of nonlinear optical liquids in the visible and near-infrared spectral region. *Optical Materials Express* **2**, 1588, https://doi.org/10.1364/ome.2.001588 (2012).
216. Kerl, K. & Varchmin, H. Refractive index dispersion (RID) of some liquids in the UV/VIS between 20 °C and 60 °C. *Journal of Molecular Structure* **349**, 257–260, https://doi.org/10.1016/0022-2860(95)08758-n (1995).
217. Kerremans, R. *et al*. The optical constants of solution-processed semiconductors—new challenges with perovskites and non-fullerene acceptors. *Advanced Optical Materials* **8**, https://doi.org/10.1002/adom.202000319 (2020).

218. Kim, Y. D. *et al*. Optical properties of zinc-blende CdSe and $Zn_xCd_{1-x}Se$ films grown on GaAs. *Physical Review B* **49**, 7262–7270, https://doi.org/10.1103/physrevb.49.7262 (1994).
219. Kischkat, J. *et al*. Mid-infrared optical properties of thin films of aluminum oxide, titanium dioxide, silicon dioxide, aluminum nitride, and silicon nitride. *Applied Optics* **51**, 6789, https://doi.org/10.1364/ao.51.006789 (2012).
220. Kitamura, R., Pilon, L. & Jonasz, M. Optical constants of silica glass from extreme ultraviolet to far infrared at near room temperature. *Applied Optics* **46**, 8118, https://doi.org/10.1364/ao.46.008118 (2007).
221. Kiyoshi Kato, K. K. & Hiromichi Shirahata, H. S. Nonlinear ir generation in $AgGaS_2$. *Japanese Journal of Applied Physics* **35**, 4645, https://doi.org/10.1143/jjap.35.4645 (1996).
222. Klein, C. A. Room-temperature dispersion equations for cubic zinc sulfide. *Applied Optics* **25**, 1873, https://doi.org/10.1364/ao.25.001873 (1986).
223. Kofman, V., He, J., Loes ten Kate, I. & Linnartz, H. The refractive index of amorphous and crystalline water ice in the UV–vis. *The Astrophysical Journal* **875**, 131, https://doi.org/10.3847/1538-4357/ab0d89 (2019).
224. Kozma, I. Z., Krok, P. & Riedle, E. Direct measurement of the group-velocity mismatch and derivation of the refractive-index dispersion for a variety of solvents in the ultraviolet. *Journal of the Optical Society of America B* **22**, 1479, https://doi.org/10.1364/josab.22.001479 (2005).
225. Krauter, P. *et al*. Optical phantoms with adjustable subdiffusive scattering parameters. *Journal of Biomedical Optics* **20**, 105008, https://doi.org/10.1117/1.jbo.20.10.105008 (2015).
226. Kulikova, D. P. *et al*. Optical properties of tungsten trioxide, palladium, and platinum thin films for functional nanostructures engineering. *Optics Express* **28**, 32049, https://doi.org/10.1364/oe.405403 (2020).
227. Kumar, A. *et al*. Linear and nonlinear optical properties of $BiFeO_3$. *Applied Physics Letters* **92**, https://doi.org/10.1063/1.2901168 (2008).
228. Laiho, R. & Lakkisto, M. Investigation of the refractive indices of LaF_3, CeF_3, PrF_3 and NdF_3. *Philosophical Magazine B* **48**, 203–207, https://doi.org/10.1080/13642818308226470 (1983).
229. Lajaunie, L., Boucher, F., Dessapt, R. & Moreau, P. Strong anisotropic influence of local-field effects on the dielectric response of α-MoO_3. *Physical Review B* **88**, https://doi.org/10.1103/physrevb.88.115141 (2013).
230. Lane, D. W. The optical properties and laser irradiation of some common glasses. *Journal of Physics D: Applied Physics* **23**, 1727–1734, https://doi.org/10.1088/0022-3727/23/12/037 (1990).
231. Larruquert, J. I., Méndez, J. A. & Aznárez, J. A. Far-ultraviolet reflectance measurements and optical constants of unoxidized aluminum films. *Applied Optics* **34**, 4892, https://doi.org/10.1364/ao.34.004892 (1995).
232. Larruquert, J. I., Méndez, J. A. & Aznárez, J. A. Optical constants of aluminum films in the extreme ultraviolet interval of 82–77 nm. *Applied Optics* **35**, 5692, https://doi.org/10.1364/ao.35.005692 (1996).
233. Larruquert, J. I., Aznárez, J. A., Méndez, J. A. & Calvo-Angós, J. Optical properties of ytterbium films in the far and the extreme ultraviolet. *Applied Optics* **42**, 4566, https://doi.org/10.1364/ao.42.004566 (2003).
234. Larruquert, J. I. *et al*. Optical properties of scandium films in the far and the extreme ultraviolet. *Applied Optics* **43**, 3271, https://doi.org/10.1364/ao.43.003271 (2004).
235. Larruquert, J. I. *et al*. Transmittance and optical constants of erbium films in the 325–1580 eV spectral range. *Applied Optics* **50**, 2211, https://doi.org/10.1364/ao.50.002211 (2011).
236. Larruquert, J. I. *et al*. Self-consistent optical constants of SiC thin films. *Journal of the Optical Society of America A* **28**, 2340, https://doi.org/10.1364/josaa.28.002340 (2011).
237. Larruquert, J. I. *et al*. Self-consistent optical constants of sputter-deposited B4C thin films. *Journal of the Optical Society of America A* **29**, 117, https://doi.org/10.1364/josaa.29.000117 (2011).
238. Larruquert, J. I., Rodríguez-de Marcos, L. V., Méndez, J. A., Martin, P. J. & Bendavid, A. High reflectance ta-C coatings in the extreme ultraviolet. *Optics Express* **21**, 27537, https://doi.org/10.1364/oe.21.027537 (2013).
239. Larsén, T. Beitrag zur dispersion der edelgase. *Zeitschrift für Physik* **88**, 389–394, https://doi.org/10.1007/bf01343498 (1934).
240. Le, T. N., Pelouard, J.-L., Charra, F. & Vassant, S. Determination of the far-infrared dielectric function of a thin InGaAs layer using a detuned Salisbury screen. *Optical Materials Express* **12**, 2711, https://doi.org/10.1364/ome.455445 (2022).
241. Lee, S., Jeong, T., Jung, S. & Yee, K. Refractive index dispersion of hexagonal boron nitride in the visible and near-infrared. *physica status solidi (b)* **256**, https://doi.org/10.1002/pssb.201800417 (2018).
242. Leguy, A. M. A. *et al*. Reversible hydration of $CH_3NH_3PbI_3$ in films, single crystals, and solar cells. *Chemistry of Materials* **27**, 3397–3407, https://doi.org/10.1021/acs.chemmater.5b00660 (2015).
243. Leite, T. R., Zschiedrich, L., Kizilkaya, O. & McPeak, K. M. Resonant plasmonic–biomolecular chiral interactions in the far-ultraviolet: Enantiomeric discrimination of sub-10 nm amino acid films. *Nano Letters* **22**, 7343–7350, https://doi.org/10.1021/acs.nanolett.2c01724 (2022).
244. Leonard, P. Refractive indices, verdet constants, and polarizabilities of the inert gases. *Atomic Data and Nuclear Data Tables* **14**, 21–37, https://doi.org/10.1016/s0092-640x(74)80028-8 (1974).
245. Li, H. H. Refractive index of alkali halides and its wavelength and temperature derivatives. *Journal of Physical and Chemical Reference Data* **5**, 329–528, https://doi.org/10.1063/1.555536 (1976).
246. Li, H. H. Refractive index of alkaline earth halides and its wavelength and temperature derivatives. *Journal of Physical and Chemical Reference Data* **9**, 161–290, https://doi.org/10.1063/1.555616 (1980).
247. Li, H. H. Refractive index of silicon and germanium and its wavelength and temperature derivatives. *Journal of Physical and Chemical Reference Data* **9**, 561–658, https://doi.org/10.1063/1.555624 (1980).
248. Li, H. H. Refractive index of ZnS, ZnSe, and ZnTe and its wavelength and temperature derivatives. *Journal of Physical and Chemical Reference Data* **13**, 103–150, https://doi.org/10.1063/1.555705 (1984).
249. Li, J., Wen, C.-H., Gauza, S., Lu, R. & Wu, S.-T. Refractive indices of liquid crystals for display applications. *Journal of Display Technology* **1**, 51–61, https://doi.org/10.1109/jdt.2005.853357 (2005).
250. Lin, M., Sverdlov, B., Strite, S., Morkoç, H. & Drakin, A. Refractive indices of wurtzite and zincblende GaN. *Electronics Letters* **29**, 1759, https://doi.org/10.1049/el:19931172 (1993).
251. Lin, Q. *et al*. Dispersion of silicon nonlinearities in the near infrared region. *Applied Physics Letters* **91**, https://doi.org/10.1063/1.2750523 (2007).
252. Lisitsa, M. P., Gudymenko, L. F., Malinko, V. N. & Terekhova, S. F. Dispersion of the refractive indices and birefringence of CdS_xSe_{1-x} single crystals. *physica status solidi (b)* **31**, 389–399, https://doi.org/10.1002/pssb.19690310146 (1969).
253. Logothetidis, S., Petalas, J., Cardona, M. & Moustakas, T. D. Optical properties and temperature dependence of the interband transitions of cubic and hexagonal GaN. *Physical Review B* **50**, 18017–18029, https://doi.org/10.1103/physrevb.50.18017 (1994).
254. Loiko, P. & Major, A. Dispersive properties of alexandrite and beryllium hexaaluminate crystals. *Optical Materials Express* **6**, 2177, https://doi.org/10.1364/ome.6.002177 (2016).
255. Loiko, P. *et al*. Sellmeier equations, group velocity dispersion, and thermo-optic dispersion formulas for $CaLnAlO_4$ (Ln = Y, Gd) laser host crystals. *Optics Letters* **42**, 2275, https://doi.org/10.1364/ol.42.002275 (2017).
256. Lomheim, T. S. & DeShazer, L. G. Optical-absorption intensities of trivalent neodymium in the uniaxial crystal yttrium orthovanadate. *Journal of Applied Physics* **49**, 5517–5522, https://doi.org/10.1063/1.324471 (1978).
257. Loria, S. Über die dispersion des lichtes in gasförmigen kohlenwasserstoffen. *Annalen der Physik* **334**, 605–622, https://doi.org/10.1002/andp.19093340809 (1909).

258. Lorimor, O. G. & Spitzer, W. G. Infrared refractive index and absorption of InAs and CdTe. *Journal of Applied Physics* **36**, 1841–1844, https://doi.org/10.1063/1.1714362 (1965).
259. Luke, K., Okawachi, Y., Lamont, M. R. E., Gaeta, A. L. & Lipson, M. Broadband mid-infrared frequency comb generation in a Si_3N_4 microresonator. *Optics Letters* **40**, 4823, https://doi.org/10.1364/ol.40.004823 (2015).
260. Magnozzi, M., Ferrera, M., Mattera, L., Canepa, M. & Bisio, F. Plasmonics of au nanoparticles in a hot thermodynamic bath. *Nanoscale* **11**, 1140–1146, https://doi.org/10.1039/c8nr09038f (2019).
261. Malitson, I. H. Refraction and dispersion of synthetic sapphire. *Journal of the Optical Society of America* **52**, 1377, https://doi.org/10.1364/josa.52.001377 (1962).
262. Malitson, I. H. A redetermination of some optical properties of calcium fluoride. *Applied Optics* **2**, 1103, https://doi.org/10.1364/ao.2.001103 (1963).
263. Malitson, I. H. Refractive properties of barium fluoride. *Journal of the Optical Society of America* **54**, 628, https://doi.org/10.1364/josa.54.000628 (1964).
264. Malitson, I. H. Interspecimen comparison of the refractive index of fused silica. *Journal of the Optical Society of America* **55**, 1205, https://doi.org/10.1364/josa.55.001205 (1965).
265. Mansfield, C. R. & Peck, E. R. Dispersion of helium. *Journal of the Optical Society of America* **59**, 199, https://doi.org/10.1364/josa.59.000199 (1969).
266. Marcos, L. R.-d. *et al*. Optical constants of SrF_2 thin films in the 25–780-eV spectral range. *Journal of Applied Physics* **113**, https://doi.org/10.1063/1.4800099 (2013).
267. Marcos, L. R.-d *et al*. Transmittance and optical constants of Ca films in the 4–1000 eV spectral range. *Applied Optics* **54**, 1910, https://doi.org/10.1364/ao.54.001910 (2015).
268. Marple, D. T. F. Refractive index of ZnSe, ZnTe, and CdTe. *Journal of Applied Physics* **35**, 539–542, https://doi.org/10.1063/1.1713411 (1964).
269. Martonchik, J. V. & Orton, G. S. Optical constants of liquid and solid methane. *Applied Optics* **33**, 8306, https://doi.org/10.1364/ao.33.008306 (1994).
270. Mathar, R. J. Refractive index of humid air in the infrared: model fits. *Journal of Optics A: Pure and Applied Optics* **9**, 470–476, https://doi.org/10.1088/1464-4258/9/5/008 (2007).
271. Mathewson, A. G. & Myers, H. P. Absolute values of the optical constants of some pure metals. *Physica Scripta* **4**, 291–292, https://doi.org/10.1088/0031-8949/4/6/009 (1971).
272. Mavrona, E. *et al*. Refractive index measurement of IP-S and IP-Dip photoresists at THz frequencies and validation via 3D photonic metamaterials made by direct laser writing. *Optical Materials Express* **13**, 3355, https://doi.org/10.1364/ome.500287 (2023).
273. McPeak, K. M. *et al*. Plasmonic films can easily be better: Rules and recipes. *ACS Photonics* **2**, 326–333, https://doi.org/10.1021/ph5004237 (2015).
274. Medenbach, O., Dettmar, D., Shannon, R. D., Fischer, R. X. & Yen, W. M. Refractive index and optical dispersion of rare earth oxides using a small-prism technique. *Journal of Optics A: Pure and Applied Optics* **3**, 174–177, https://doi.org/10.1088/1464-4258/3/3/303 (2001).
275. Meretska, M. L. *et al*. Measurements of the magneto-optical properties of thin-film EuS at room temperature in the visible spectrum. *Applied Physics Letters* **120**, https://doi.org/10.1063/5.0090533 (2022).
276. Milam, D., Weber, M. J. & Glass, A. J. Nonlinear refractive index of fluoride crystals. *Applied Physics Letters* **31**, 822–825, https://doi.org/10.1063/1.89561 (1977).
277. Milam, D. Review and assessment of measured values of the nonlinear refractive-index coefficient of fused silica. *Applied Optics* **37**, 546, https://doi.org/10.1364/ao.37.000546 (1998).
278. Miller, S. *et al*. Polarization-dependent nonlinear refractive index of BiB_3O_6. *Optical Materials* **30**, 1469–1472, https://doi.org/10.1016/j.optmat.2007.11.015 (2008).
279. Moerland, R. J. & Hoogenboom, J. P. Subnanometer-accuracy optical distance ruler based on fluorescence quenching by transparent conductors. *Optica* **3**, 112, https://doi.org/10.1364/optica.3.000112 (2016).
280. Monin, J. & Boutry, G. A. Optical and photoelectric properties of alkali metals. *Physical Review B* **9**, 1309–1327, https://doi.org/10.1103/physrevb.9.1309 (1974).
281. Moutzouris, K., Hloupis, G., Stavrakas, I., Triantis, D. & Chou, M.-H. Temperature-dependent visible to near-infrared optical properties of 8 mol% Mg-doped lithium tantalate. *Optical Materials Express* **1**, 458, https://doi.org/10.1364/ome.1.000458 (2011).
282. Moutzouris, K., Stavrakas, I., Triantis, D. & Enculescu, M. Temperature-dependent refractive index of potassium acid phthalate (KAP) in the visible and near-infrared. *Optical Materials* **33**, 812–816, https://doi.org/10.1016/j.optmat.2010.12.021 (2011).
283. Moutzouris, K. *et al*. Refractive, dispersive and thermo-optic properties of twelve organic solvents in the visible and near-infrared. *Applied Physics B* **116**, 617–622, https://doi.org/10.1007/s00340-013-5744-3 (2013).
284. Munkhbat, B., Wróbel, P., Antosiewicz, T. J. & Shegai, T. O. Optical constants of several multilayer transition metal dichalcogenides measured by spectroscopic ellipsometry in the 300–1700 nm range: High index, anisotropy, and hyperbolicity. *ACS Photonics* **9**, 2398–2407, https://doi.org/10.1021/acsphotonics.2c00433 (2022).
285. Myers, T. L. *et al*. Accurate measurement of the optical constants n and k for a series of 57 inorganic and organic liquids for optical modeling and detection. *Applied Spectroscopy* **72**, 535–550, https://doi.org/10.1177/0003702817742848 (2017).
286. Nibbering, E. T. J., Grillon, G., Franco, M. A., Prade, B. S. & Mysyrowicz, A. Determination of the inertial contribution to the nonlinear refractive index of air, N_2, and O_2 by use of unfocused high-intensity femtosecond laser pulses. *Journal of the Optical Society of America B* **14**, 650, https://doi.org/10.1364/josab.14.000650 (1997).
287. Nigara, Y. Measurement of the optical constants of yttrium oxide. *Japanese Journal of Applied Physics* **7**, 404, https://doi.org/10.1143/jjap.7.404 (1968).
288. Ninomiya, S. & Adachi, S. Optical properties of wurtzite CdS. *Journal of Applied Physics* **78**, 1183–1190, https://doi.org/10.1063/1.360355 (1995).
289. Ninomiya, S. & Adachi, S. Optical properties of cubic and hexagonal CdSe. *Journal of Applied Physics* **78**, 4681–4689, https://doi.org/10.1063/1.359815 (1995).
290. Nunley, T. N. *et al*. Optical constants of germanium and thermally grown germanium dioxide from 0.5 to 6.6 eV via a multisample ellipsometry investigation. *Journal of Vacuum Science & Technology B, Nanotechnology and Microelectronics: Materials, Processing, Measurement, and Phenomena* **34**, https://doi.org/10.1116/1.4963075 (2016).
291. Nyakuchena, M., Juntunen, C., Shea, P. & Sung, Y. Refractive index dispersion measurement in the short-wave infrared range using synthetic phase microscopy. *Physical Chemistry Chemical Physics* **25**, 23141–23149, https://doi.org/10.1039/d3cp03158f (2023).
292. Oguntoye, I. O. *et al*. Continuously tunable optical modulation using vanadium dioxide huygens metasurfaces. *ACS Applied Materials & Interfaces* **15**, 41141–41150, https://doi.org/10.1021/acsami.3c08493 (2023).
293. Old, J. G., Gentili, K. L. & Peck, E. R. Dispersion of carbon dioxide. *Journal of the Optical Society of America* **61**, 89, https://doi.org/10.1364/josa.61.000089 (1971).
294. Olmon, R. L. *et al*. Optical dielectric function of gold. *Physical Review B* **86**, https://doi.org/10.1103/physrevb.86.235147 (2012).
295. Ordal, M. A., Bell, R. J., Alexander, R. W., Long, L. L. & Querry, M. R. Optical properties of fourteen metals in the infrared and far infrared: Al, Co, Cu, Au, Fe, Pb, Mo, Ni, Pd, Pt, Ag, Ti, V, and W. *Applied Optics* **24**, 4493, https://doi.org/10.1364/ao.24.004493 (1985).
296. Ordal, M. A., Bell, R. J., Alexander, R. W., Long, L. L. & Querry, M. R. Optical properties of Au, Ni, and Pb at submillimeter wavelengths. *Applied Optics* **26**, 744, https://doi.org/10.1364/ao.26.000744 (1987).

297. Ordal, M. A., Bell, R. J., Alexander, R. W., Newquist, L. A. & Querry, M. R. Optical properties of Al, Fe, Ti, Ta, W, and Mo at submillimeter wavelengths. *Applied Optics* **27**, 1203, https://doi.org/10.1364/ao.27.001203 (1988).
298. Otanicar, T. P., Phelan, P. E. & Golden, J. S. Optical properties of liquids for direct absorption solar thermal energy systems. *Solar Energy* **83**, 969–977, https://doi.org/10.1016/j.solener.2008.12.009 (2009).
299. Owyoung, A. Ellipse rotation studies in laser host materials. *IEEE Journal of Quantum Electronics* **9**, 1064–1069, https://doi.org/10.1109/jqe.1973.1077417 (1973).
300. Ozaki, S. & Adachi, S. Spectroscopic ellipsometry and thermoreflectance of GaAs. *Journal of Applied Physics* **78**, 3380–3386, https://doi.org/10.1063/1.359966 (1995).
301. Palm, K. J., Murray, J. B., Narayan, T. C. & Munday, J. N. Dynamic optical properties of metal hydrides. *ACS Photonics* **5**, 4677–4686, https://doi.org/10.1021/acsphotonics.8b01243 (2018).
302. Panah, M. E. A. *et al*. Highly doped inp as a low loss plasmonic material for mid-IR region. *Optics Express* **24**, 29077, https://doi.org/10.1364/oe.24.029077 (2016).
303. Papatryfonos, K. *et al*. Refractive indices of mbe-grown $Al_xGa_{(1-x)}As$ ternary alloys in the transparent wavelength region. *AIP Advances* **11**, https://doi.org/10.1063/5.0039631 (2021).
304. Parsons, D. F. & Coleman, P. D. Far infrared optical constants of gallium phosphide. *Applied Optics* **10**, 1683, https://doi.org/10.1364/ao.10.1683_1 (1971).
305. Pastrňák, J. & Roskovcová, L. Refraction index measurements on AlN single crystals. *physica status solidi (b)* **14**, https://doi.org/10.1002/pssb.19660140127 (1966).
306. Patwardhan, G. N., Ginsberg, J. S., Chen, C. Y., Jadidi, M. M. & Gaeta, A. L. Nonlinear refractive index of solids in mid-infrared. *Optics Letters* **46**, 1824, https://doi.org/10.1364/ol.421469 (2021).
307. Peck, E. R. & Fisher, D. J. Dispersion of argon. *Journal of the Optical Society of America* **54**, 1362, https://doi.org/10.1364/josa.54.001362 (1964).
308. Peck, E. R. & Khanna, B. N. Dispersion of nitrogen. *Journal of the Optical Society of America* **56**, 1059, https://doi.org/10.1364/josa.56.001059 (1966).
309. Peck, E. R. & Reeder, K. Dispersion of air. *Journal of the Optical Society of America* **62**, 958, https://doi.org/10.1364/josa.62.000958 (1972).
310. Peck, E. R. & Huang, S. Refractivity and dispersion of hydrogen in the visible and near infrared. *Journal of the Optical Society of America* **67**, 1550, https://doi.org/10.1364/josa.67.001550 (1977).
311. Pennington, D. M., Henesian, M. A. & Hellwarth, R. W. Nonlinear index of air at 1.053 μm. *Physical Review A* **39**, 3003–3009, https://doi.org/10.1103/physreva.39.3003 (1989).
312. Perner, L. W. *et al*. Simultaneous measurement of mid-infrared refractive indices in thin-film heterostructures: Methodology and results for GaAs/AlGaAs. *Physical Review Research* **5**, https://doi.org/10.1103/physrevresearch.5.033048 (2023).
313. Perotto, G. *et al*. The optical properties of regenerated silk fibroin films obtained from different sources. *Applied Physics Letters* **111**, https://doi.org/10.1063/1.4998950 (2017).
314. Pestryakov, E. V. *et al*. Physical properties of $BeAl_6O_{10}$ single crystals. *Journal of Applied Physics* **82**, 3661–3666, https://doi.org/10.1063/1.365728 (1997).
315. Peter, F. Über brechungsindizes und absorptionskonstanten des diamanten zwischen 644 und 226 mμ. *Zeitschrift für Physik* **15**, 358–368, https://doi.org/10.1007/bf01330487 (1923).
316. Pettit, G. D. & Turner, W. J. Refractive index of InP. *Journal of Applied Physics* **36**, 2081–2081, https://doi.org/10.1063/1.1714410 (1965).
317. Pflüger, J., Fink, J., Weber, W., Bohnen, K. P. & Crecelius, G. Dielectric properties of TiC_x, TiN_x, VC_x, and VN_x from 1.5 to 40 eV determined by electron-energy-loss spectroscopy. *Physical Review B* **30**, 1155–1163, https://doi.org/10.1103/physrevb.30.1155 (1984).
318. Philipp, H. R. Optical properties of silicon nitride. *Journal of The Electrochemical Society* **120**, 295, https://doi.org/10.1149/1.2403440 (1973).
319. Philipp, H. R., Cole, H. S., Liu, Y. S. & Sitnik, T. A. Optical absorption of some polymers in the region 240–170 nm. *Applied Physics Letters* **48**, 192–194, https://doi.org/10.1063/1.96940 (1986).
320. Phillip, H. R. & Taft, E. A. Kramers-Kronig analysis of reflectance data for diamond. *Physical Review* **136**, A1445–A1448, https://doi.org/10.1103/physrev.136.a1445 (1964).
321. Phillips, L. J. *et al*. Dispersion relation data for methylammonium lead triiodide perovskite deposited on a (100) silicon wafer using a two-step vapour-phase reaction process. *Data in Brief* **5**, 926–928, https://doi.org/10.1016/j.dib.2015.10.026 (2015).
322. Pierce, D. T. & Spicer, W. E. Electronic structure of amorphous Si from photoemission and optical studies. *Physical Review B* **5**, 3017–3029, https://doi.org/10.1103/physrevb.5.3017 (1972).
323. Pigeon, J. J., Tochitsky, S. Y., Welch, E. C. & Joshi, C. Measurements of the nonlinear refractive index of air, N_2, and O_2 at 10 μm using four-wave mixing. *Optics Letters* **41**, 3924, https://doi.org/10.1364/ol.41.003924 (2016).
324. Pigeon, J. J., Matteo, D. A., Tochitsky, S. Y., Ben-Zvi, I. & Joshi, C. Measurements of the nonlinear refractive index of $AgGaSe_2$, GaSe, and ZnSe at 10 μm. *Journal of the Optical Society of America B* **37**, 2076, https://doi.org/10.1364/josab.395844 (2020).
325. Polyanskiy, M. N. *et al*. Single-shot measurement of the nonlinear refractive index of air at 9.2 μm with a picosecond terawatt CO_2 laser. *Optics Letters* **46**, 2067, https://doi.org/10.1364/ol.423800 (2021).
326. Polyanskiy, M. N. *et al*. Post-compression of long-wave infrared 2 picosecond sub-terawatt pulses in bulk materials. *Optics Express* **29**, 31714, https://doi.org/10.1364/oe.434238 (2021).
327. Radhakrishnan, T. The dispersion, briefringence and optical activity of quartz. *Proceedings of the Indian Academy of Sciences - Section A* **25**, https://doi.org/10.1007/bf03171408 (1947).
328. Radhakrishnan, T. Further studies on the temperature variation of the refractive index of crystals. *Proceedings of the Indian Academy of Sciences - Section A* **33**, https://doi.org/10.1007/bf03172255 (1951).
329. Rakić, A. D. Algorithm for the determination of intrinsic optical constants of metal films: application to aluminum. *Applied Optics* **34**, 4755, https://doi.org/10.1364/ao.34.004755 (1995).
330. Rakić, A. D. & Majewski, M. L. Modeling the optical dielectric function of GaAs and AlAs: Extension of Adachi's model. *Journal of Applied Physics* **80**, 5909–5914, https://doi.org/10.1063/1.363586 (1996).
331. Rakić, A. D., Djurišić, A. B., Elazar, J. M. & Majewski, M. L. Optical properties of metallic films for vertical-cavity optoelectronic devices. *Applied Optics* **37**, 5271, https://doi.org/10.1364/ao.37.005271 (1998).
332. Rasigni, M. & Rasigni, G. Optical constants of lithium deposits as determined from the Kramers-Kronig analysis. *Journal of the Optical Society of America* **67**, 54, https://doi.org/10.1364/josa.67.000054 (1977).
333. Ratzsch, S., Kley, E.-B., Tünnermann, A. & Szeghalmi, A. Influence of the oxygen plasma parameters on the atomic layer deposition of titanium dioxide. *Nanotechnology* **26**, 024003, https://doi.org/10.1088/0957-4484/26/2/024003 (2014).
334. Rheims, J., Köser, J. & Wriedt, T. Refractive-index measurements in the near-IR using an Abbe refractometer. *Measurement Science and Technology* **8**, 601–605, https://doi.org/10.1088/0957-0233/8/6/003 (1997).
335. Rioux, D. *et al*. An analytic model for the dielectric function of Au, Ag, and their alloys. *Advanced Optical Materials* **2**, 176–182, https://doi.org/10.1002/adom.201300457 (2013).
336. Rodney, W. S. Optical properties of cesium iodide. *Journal of the Optical Society of America* **45**, 987, https://doi.org/10.1364/josa.45.000987 (1955).

337. Rodney, W. S. & Malitson, I. H. Refraction and dispersion of thallium bromide iodide. *Journal of the Optical Society of America* **46**, 956, https://doi.org/10.1364/josa.46.000956 (1956).
338. Rodney, W. S., Malitson, I. H. & King, T. A. Refractive index of arsenic trisulfide. *Journal of the Optical Society of America* **48**, 633, https://doi.org/10.1364/josa.48.000633 (1958).
339. Rodríguez-de Marcos, L. *et al*. Transmittance and optical constants of Sr films in the 6–1220 eV spectral range. *Journal of Applied Physics* **111**, https://doi.org/10.1063/1.4729487 (2012).
340. Rodríguez-de Marcos, L. V., Larruquert, J. I., Méndez, J. A. & Aznárez, J. A. Self-consistent optical constants of SiO_2 and Ta_2O_5 films. *Optical Materials Express* **6**, 3622, https://doi.org/10.1364/ome.6.003622 (2016).
341. Rodríguez-de Marcos, L. V., Larruquert, J. I., Méndez, J. A. & Aznárez, J. A. Self-consistent optical constants of MgF_2, LaF_3, and CeF_3 films. *Optical Materials Express* **7**, 989, https://doi.org/10.1364/ome.7.000989 (2017).
342. Rollefson, R. & Havens, R. Index of refraction of methane in the infra-red and the dipole moment of the CH bond. *Physical Review* **57**, 710–717, https://doi.org/10.1103/physrev.57.710 (1940).
343. Rosenblatt, G., Simkhovich, B., Bartal, G. & Orenstein, M. Nonmodal plasmonics: Controlling the forced optical response of nanostructures. *Physical Review X* **10**, https://doi.org/10.1103/physrevx.10.011071 (2020).
344. Rosker, M., Cheng, K. & Tang, C. Practical urea optical parametric oscillator for tunable generation throughout the visible and near-infrared. *IEEE Journal of Quantum Electronics* **21**, 1600–1606, https://doi.org/10.1109/jqe.1985.1072557 (1985).
345. Rowe, D. J., Smith, D. & Wilkinson, J. S. Complex refractive index spectra of whole blood and aqueous solutions of anticoagulants, analgesics and buffers in the mid-infrared. *Scientific Reports* **7**, https://doi.org/10.1038/s41598-017-07842-0 (2017).
346. Rowe, P. M., Fergoda, M. & Neshyba, S. Temperature-dependent optical properties of liquid water from 240 to 298 K. *Journal of Geophysical Research: Atmospheres* **125**, https://doi.org/10.1029/2020jd032624 (2020).
347. Rubin, M. Optical properties of soda lime silica glasses. *Solar Energy Materials* **12**, 275–288, https://doi.org/10.1016/0165-1633(85)90052-8 (1985).
348. Sahin, S., Nahar, N. K. & Sertel, K. Dielectric properties of low-loss polymers for mmw and THz applications. *Journal of Infrared, Millimeter, and Terahertz Waves* **40**, 557–573, https://doi.org/10.1007/s10762-019-00584-2 (2019).
349. Salzberg, C. D. & Villa, J. J. Infrared refractive indexes of silicon germanium and modified selenium glass. *Journal of the Optical Society of America* **47**, 244, https://doi.org/10.1364/josa.47.000244 (1957).
350. Sani, E. & Dell'Oro, A. Optical constants of ethylene glycol over an extremely wide spectral range. *Optical Materials* **37**, 36–41, https://doi.org/10.1016/j.optmat.2014.04.035 (2014).
351. Sani, E. & Dell'Oro, A. Corrigendum to "Optical constants of ethylene glycol over an extremely wide spectral range [opt. mater. 37 (2014) 36–41]. *Optical Materials* **48**, 281, https://doi.org/10.1016/j.optmat.2015.06.039 (2015).
352. Sani, E. & Dell'Oro, A. Spectral optical constants of ethanol and isopropanol from ultraviolet to far infrared. *Optical Materials* **60**, 137–141, https://doi.org/10.1016/j.optmat.2016.06.041 (2016).
353. Sarkar, S. *et al*. Hybridized guided-mode resonances via colloidal plasmonic self-assembled grating. *ACS Applied Materials & Interfaces* **11**, 13752–13760, https://doi.org/10.1021/acsami.8b20535 (2019).
354. Sarkar, S. *et al*. Enhanced figure of merit via hybridized guided-mode resonances in 2*d*-metallic photonic crystal slabs. *Advanced Optical Materials* **10**, https://doi.org/10.1002/adom.202200954 (2022).
355. Sasaki, T., Mori, Y. & Yoshimura, M. Progress in the growth of a $CsLiB_6O_{10}$ crystal and its application to ultraviolet light generation. *Optical Materials* **23**, 343–351, https://doi.org/10.1016/s0925-3467(02)00316-6 (2003).
356. Sato, K. & Adachi, S. Optical properties of ZnTe. *Journal of Applied Physics* **73**, 926–931, https://doi.org/10.1063/1.353305 (1993).
357. Schinke, C., Hinken, D., Schmidt, J., Bothe, K. & Brendel, R. Modeling the spectral luminescence emission of silicon solar cells and wafers. *IEEE Journal of Photovoltaics* **3**, 1038–1052, https://doi.org/10.1109/jphotov.2013.2263985 (2013).
358. Schinke, C. *et al*. Uncertainty analysis for the coefficient of band-to-band absorption of crystalline silicon. *AIP Advances* **5**, https://doi.org/10.1063/1.4923379 (2015).
359. Schmitt, P. *et al*. Optical, structural, and functional properties of highly reflective and stable iridium mirror coatings for infrared applications. *Optical Materials Express* **12**, 545, https://doi.org/10.1364/ome.447306 (2022).
360. Schnabel, V., Spolenak, R., Doebeli, M. & Galinski, H. Structural color sensors with thermal memory: Measuring functional properties of Ti-based nitrides by eye. *Advanced Optical Materials* **6**, https://doi.org/10.1002/adom.201800656 (2018).
361. Schneider, F., Draheim, J., Kamberger, R. & Wallrabe, U. Process and material properties of polydimethylsiloxane (PDMS) for optical MEMS. *Sensors and Actuators A: Physical* **151**, 95–99, https://doi.org/10.1016/j.sna.2009.01.026 (2009).
362. Schnepf, M. J. *et al*. Nanorattles with tailored electric field enhancement. *Nanoscale* **9**, 9376–9385, https://doi.org/10.1039/c7nr02952g (2017).
363. Schröter, H. Über die brechungsindizes einiger schwermetallhalogenide im sichtbaren und die berechnung von interpolationsformeln für den dispersionsverlauf. *Zeitschrift für Physik* **67**, 24–36, https://doi.org/10.1007/bf01391040 (1931).
364. Schubert, M. *et al*. Optical constants of $Ga_xIn_{1-x}P$ lattice matched to GaAs. *Journal of Applied Physics* **77**, 3416–3419, https://doi.org/10.1063/1.358632 (1995).
365. Seçkin, S., Singh, P., Jaiswal, A. & König, T. A. F. Super-radiant sers enhancement by plasmonic particle gratings. *ACS Applied Materials & Interfaces* **15**, 43124–43134, https://doi.org/10.1021/acsami.3c07532 (2023).
366. Selivanov, A., Denisov, I., Kuleshov, N. & Yumashev, K. Nonlinear refractive properties of Yb^{3+}-doped $KY(WO_4)_2$ and YVO_4 laser crystals. *Applied Physics B* **83**, 61–65, https://doi.org/10.1007/s00340-005-2098-5 (2006).
367. Shaffer, P. T. B. Refractive index, dispersion, and birefringence of silicon carbide polytypes. *Applied Optics* **10**, 1034, https://doi.org/10.1364/ao.10.001034 (1971).
368. Shaw, M., Hooker, C. & Wilson, D. Measurement of the nonlinear refractive index of air and other gases at 248 nm. *Optics Communications* **103**, 153–160, https://doi.org/10.1016/0030-4018(93)90657-q (1993).
369. Sheik-Bahae, M., Hutchings, D., Hagan, D. & Van Stryland, E. Dispersion of bound electron nonlinear refraction in solids. *IEEE Journal of Quantum Electronics* **27**, 1296–1309, https://doi.org/10.1109/3.89946 (1991).
370. Shimoji, Y., Fay, A. T., Chang, R. S. F. & Djeu, N. Direct measurement of the nonlinear refractive index of air. *Journal of the Optical Society of America B* **6**, 1994, https://doi.org/10.1364/josab.6.001994 (1989).
371. Shkondin, E., Repän, T., Takayama, O. & Lavrinenko, A. V. High aspect ratio titanium nitride trench structures as plasmonic biosensor. *Optical Materials Express* **7**, 4171, https://doi.org/10.1364/ome.7.004171 (2017).
372. Shkondin, E. *et al*. Large-scale high aspect ratio Al-doped ZnO nanopillars arrays as anisotropic metamaterials. *Optical Materials Express* **7**, 1606, https://doi.org/10.1364/ome.7.001606 (2017).
373. Shunji Ozaki, S. O. & Sadao Adachi, S. A. Optical constants of cubic ZnS. *Japanese Journal of Applied Physics* **32**, 5008, https://doi.org/10.1143/jjap.32.5008 (1993).
374. Siefke, T. *et al*. Materials pushing the application limits of wire grid polarizers further into the deep ultraviolet spectral range. *Advanced Optical Materials* **4**, 1780–1786, https://doi.org/10.1002/adom.201600250 (2016).
375. Šik, J., Hora, J. & Humlíček, J. Optical functions of silicon at high temperatures. *Journal of Applied Physics* **84**, 6291–6298, https://doi.org/10.1063/1.368951 (1998).
376. Simon, M. *et al*. Refractive indices of photorefractive bismuth titanate, barium-calcium titanate, bismuth germanium oxide, and lead germanate. *physica status solidi (a)* **159**, 559–562, 10.1002/1521-396x(199702)159:2<559::aid-pssa559>3.0.co;2-0 (1997).
377. Singh, S., Potopowicz, J. R., Van Uitert, L. G. & Wemple, S. H. Nonlinear optical properties of hexagonal silicon carbide. *Applied Physics Letters* **19**, 53–56, https://doi.org/10.1063/1.1653819 (1971).

378. Singh, S., Remeika, J. P. & Potopowicz, J. R. Nonlinear optical properties of ferroelectric lead titanate. *Applied Physics Letters* **20**, 135–137, https://doi.org/10.1063/1.1654078 (1972).
379. Sinnock, A. C. & Smith, B. L. Refractive indices of the condensed inert gases. *Physical Review* **181**, 1297–1307, https://doi.org/10.1103/physrev.181.1297 (1969).
380. Skauli, T. *et al*. Improved dispersion relations for gaas and applications to nonlinear optics. *Journal of Applied Physics* **94**, 6447–6455, https://doi.org/10.1063/1.1621740 (2003).
381. Smith, N. V. Optical constants of sodium and potassium from 0.5 to 4.0 eV by split-beam ellipsometry. *Physical Review* **183**, 634–644, https://doi.org/10.1103/physrev.183.634 (1969).
382. Smith, N. V. Optical constants of rubidium and cesium from 0.5 to 4.0 eV. *Physical Review B* **2**, 2840–2848, https://doi.org/10.1103/physrevb.2.2840 (1970).
383. Smith, D. R. & Loewenstein, E. V. Optical constants of far infrared materials 3: plastics. *Applied Optics* **14**, 1335, https://doi.org/10.1364/ao.14.001335 (1975).
384. Smith, P. L., Huber, M. C. E. & Parkinson, W. H. Refractivities of H_2, He, O_2, CO, and Kr for $168 \leq \lambda \leq 288$ nm. *Physical Review A* **13**, 1422–1434, https://doi.org/10.1103/physreva.13.1422 (1976).
385. Smith, F. W. Optical constants of a hydrogenated amorphous carbon film. *Journal of Applied Physics* **55**, 764–771, https://doi.org/10.1063/1.333135 (1984).
386. Sneep, M. & Ubachs, W. Direct measurement of the Rayleigh scattering cross section in various gases. *Journal of Quantitative Spectroscopy and Radiative Transfer* **92**, 293–310, https://doi.org/10.1016/j.jqsrt.2004.07.025 (2005).
387. Song, B. *et al*. Layer-dependent dielectric function of wafer-scale 2D MoS_2. *Advanced Optical Materials* **7**, https://doi.org/10.1002/adom.201801250 (2018).
388. Song, B. *et al*. Broadband optical properties of graphene and hopg investigated by spectroscopic Mueller matrix ellipsometry. *Applied Surface Science* **439**, 1079–1087, https://doi.org/10.1016/j.apsusc.2018.01.051 (2018).
389. Song, B. *et al*. Determination of dielectric functions and exciton oscillator strength of two-dimensional hybrid perovskites. *ACS Materials Letters* **3**, 148–159, https://doi.org/10.1021/acsmaterialslett.0c00505 (2020).
390. Song, B. *et al*. Giant gate-tunability of complex refractive index in semiconducting carbon nanotubes. *ACS Photonics* **7**, 2896–2905, https://doi.org/10.1021/acsphotonics.0c01220 (2020).
391. Stahrenberg, K. *et al*. Optical properties of copper and silver in the energy range 2.5–9.0 eV. *Physical Review B* **64**, https://doi.org/10.1103/physrevb.64.115111 (2001).
392. Stefaniuk, T. *et al*. Optical, electronic, and structural properties of $ScAlMgO_4$. *Physical Review B* **107**, https://doi.org/10.1103/physrevb.107.085205 (2023).
393. Stelling, C. *et al*. Plasmonic nanomeshes: their ambivalent role as transparent electrodes in organic solar cells. *Scientific Reports* **7**, https://doi.org/10.1038/srep42530 (2017).
394. Stephens, R. & Malitson, I. Index of refraction of magnesium oxide. *Journal of Research of the National Bureau of Standards* **49**, 249, https://doi.org/10.6028/jres.049.025 (1952).
395. Supansomboon, S., Maaroof, A. & Cortie, M. B. "purple glory": The optical properties and technology of $AuAl_2$ coatings. *Gold Bulletin* **41**, 296–304, https://doi.org/10.1007/bf03214887 (2008).
396. Sutherland, J. C. & Arakawa, E. T. Optical properties of potassium for photons of energy 396 to 969 eV. *Journal of the Optical Society of America* **58**, 1080, https://doi.org/10.1364/josa.58.001080 (1968).
397. Suzuki, N., Sawai, K. & Adachi, S. Optical properties of PbSe. *Journal of Applied Physics* **77**, 1249–1255, https://doi.org/10.1063/1.358926 (1995).
398. Svechnikov, M. *et al*. Optical constants of sputtered beryllium thin films determined from photoabsorption measurements in the spectral range 20.4–250 eV. *Journal of Synchrotron Radiation* **27**, 75–82, https://doi.org/10.1107/s1600577519014188 (2020).
399. Sytchkova, A., Belosludtsev, A., Volosevičienė, L., Juškėnas, R. & Simniškis, R. Optical, structural and electrical properties of sputtered ultrathin chromium films. *Optical Materials* **121**, 111530, https://doi.org/10.1016/j.optmat.2021.111530 (2021).
400. Takaoka, E. & Kato, K. Thermo-optic dispersion formula for $AgGaS_2$. *Applied Optics* **38**, 4577, https://doi.org/10.1364/ao.38.004577 (1999).
401. Tamošauskas, G., Beresnevičius, G., Gadonas, D. & Dubietis, A. Transmittance and phase matching of BBO crystal in the 3–5 μm range and its application for the characterization of mid-infrared laser pulses. *Optical Materials Express* **8**, 1410, https://doi.org/10.1364/ome.8.001410 (2018).
402. Tan, C. Determination of refractive index of silica glass for infrared wavelengths by IR spectroscopy. *Journal of Non-Crystalline Solids* **223**, 158–163, https://doi.org/10.1016/s0022-3093(97)00438-9 (1998).
403. Tatian, B. Fitting refractive-index data with the Sellmeier dispersion formula. *Applied Optics* **23**, 4477, https://doi.org/10.1364/ao.23.004477 (1984).
404. Taylor, A. *et al*. Comparative determination of atomic boron and carrier concentration in highly boron doped nano-crystalline diamond. *Diamond and Related Materials* **135**, 109837, https://doi.org/10.1016/j.diamond.2023.109837 (2023).
405. Tikuišis, K. K. *et al*. Optical and magneto-optical properties of permalloy thin films in 0.7–6.4 eV photon energy range. *Materials & Design* **114**, 31–39, https://doi.org/10.1016/j.matdes.2016.10.036 (2017).
406. Tikuišis, K. K. *et al*. Dielectric function of epitaxial quasi-freestanding monolayer graphene on Si-face 6H-SiC in a broad spectral range. *Physical Review Materials* **7**, https://doi.org/10.1103/physrevmaterials.7.044201 (2023).
407. Tilton, L. W., Plyler, E. K. & Stephens, R. E. Refractive index of silver chloride for visible and infra-red radiant energy. *Journal of the Optical Society of America* **40**, 540, https://doi.org/10.1364/josa.40.000540 (1950).
408. Tkachenko, V. *et al*. Nematic liquid crystal optical dispersion in the visible-near infrared range. *Molecular Crystals and Liquid Crystals* **454**, 263/[665]–271/[673], https://doi.org/10.1080/15421400600655816 (2006).
409. Treharne, R. E. *et al*. Optical design and fabrication of fully sputtered CdTe/CdS solar cells. *Journal of Physics: Conference Series* **286**, 012038, https://doi.org/10.1088/1742-6596/286/1/012038 (2011).
410. Tsuda, S., Yamaguchi, S., Kanamori, Y. & Yugami, H. Spectral and angular shaping of infrared radiation in a polymer resonator with molecular vibrational modes. *Optics Express* **26**, 6899, https://doi.org/10.1364/oe.26.006899 (2018).
411. Uchida, N. Optical properties of single-crystal paratellurite (TeO_2). *Physical Review B* **4**, 3736–3745, https://doi.org/10.1103/physrevb.4.3736 (1971).
412. Umegaki, S., Tanaka, S.-I., Uchiyama, T. & Yabumoto, S. Refractive indices of lithium iodate between 0.4 and 2.2 μ. *Optics Communications* **3**, 244–245, https://doi.org/10.1016/0030-4018(71)90013-7 (1971).
413. Valentine, J. *et al*. Three-dimensional optical metamaterial with a negative refractive index. *Nature* **455**, 376–379, https://doi.org/10.1038/nature07247 (2008).
414. Vidal-Dasilva, M. *et al*. Transmittance and optical constants of Tm films in the 2.75–1600 eV spectral range. *Journal of Applied Physics* **105**, https://doi.org/10.1063/1.3129507 (2009).
415. Vidal-Dasilva, M., Aquila, A. L., Gullikson, E. M., Salmassi, F. & Larruquert, J. I. Optical constants of magnetron-sputtered magnesium films in the 25–1300 eV energy range. *Journal of Applied Physics* **108**, https://doi.org/10.1063/1.3481457 (2010).
416. Vogt, M. R. *et al*. Measurement of the optical constants of soda-lime glasses in dependence of iron content and modeling of iron-related power losses in crystalline si solar cell modules. *IEEE Journal of Photovoltaics* **6**, 111–118, https://doi.org/10.1109/jphotov.2015.2498043 (2016).

417. Vogt, M. R. *et al*. Optical constants of UV transparent EVA and the impact on the PV module output power under realistic irradiation. *Energy Procedia* **92**, 523–530, https://doi.org/10.1016/j.egypro.2016.07.136 (2016).
418. Vos, M. F. J., Macco, B., Thissen, N. F. W., Bol, A. A. & Kessels, W. M. M. E. Atomic layer deposition of molybdenum oxide from $(N^tBu)_2(NMe_2)_2Mo$ and O_2 plasma. *Journal of Vacuum Science & Technology A: Vacuum, Surfaces, and Films* **34**, https://doi.org/10.1116/1.4930161 (2015).
419. Vuković, D., Woolsey, G. A. & Scelsi, G. B. Refractivities of SF_6 and SOF_2 at wavelengths of 632.99 and 1300 nm. *Journal of Physics D: Applied Physics* **29**, 634–637, https://doi.org/10.1088/0022-3727/29/3/023 (1996).
420. Vuye, G. *et al*. Temperature dependence of the dielectric function of silicon using in situ spectroscopic ellipsometry. *Thin Solid Films* **233**, 166–170, https://doi.org/10.1016/0040-6090(93)90082-z (1993).
421. Wahlstrand, J. K., Cheng, Y.-H. & Milchberg, H. M. Absolute measurement of the transient optical nonlinearity in N_2, O_2, N_2O, and Ar. *Physical Review A* **85**, https://doi.org/10.1103/physreva.85.043820 (2012).
422. Walling, J., Peterson, O., Jenssen, H., Morris, R. & O'Dell, E. Tunable alexandrite lasers. *IEEE Journal of Quantum Electronics* **16**, 1302–1315, https://doi.org/10.1109/jqe.1980.1070430 (1980).
423. Wang, S. *et al*. 4H-SiC: a new nonlinear material for midinfrared lasers. *Laser & Photonics Reviews* **7**, 831–838, https://doi.org/10.1002/lpor.201300068 (2013).
424. Wang, Y. *et al*. Measurement of absorption spectrum of deuterium oxide (D_2O) and its application to signal enhancement in multiphoton microscopy at the 1700-nm window. *Applied Physics Letters* **108**, https://doi.org/10.1063/1.4939970 (2016).
425. Wang, K. *et al*. Order-of-magnitude multiphoton signal enhancement based on characterization of absorption spectra of immersion oils at the 1700-nm window. *Optics Express* **25**, 5909, https://doi.org/10.1364/oe.25.005909 (2017).
426. Wang, C. C., Tan, J. Y., Jing, C. Y. & Liu, L. H. Temperature-dependent optical constants of liquid isopropanol, n-butanol, and n-decane. *Applied Optics* **57**, 3003, https://doi.org/10.1364/ao.57.003003 (2018).
427. Warren, S. G. Optical constants of ice from the ultraviolet to the microwave. *Applied Optics* **23**, 1206, https://doi.org/10.1364/ao.23.001206 (1984).
428. Warren, S. G. & Brandt, R. E. Optical constants of ice from the ultraviolet to the microwave: A revised compilation. *Journal of Geophysical Research: Atmospheres* **113**, https://doi.org/10.1029/2007jd009744 (2008).
429. Weaver, J. H., Lynch, D. W. & Olson, C. G. Optical properties of niobium from 0.1 to 36.4 eV. *Physical Review B* **7**, 4311–4318, https://doi.org/10.1103/physrevb.7.4311 (1973).
430. Weaver, J. H., Olson, C. G. & Lynch, D. W. Optical properties of crystalline tungsten. *Physical Review B* **12**, 1293–1297, https://doi.org/10.1103/physrevb.12.1293 (1975).
431. Weaver, J. H., Olson, C. G. & Lynch, D. W. Optical investigation of the electronic structure of bulk Rh and Ir. *Physical Review B* **15**, 4115–4118, https://doi.org/10.1103/physrevb.15.4115 (1977).
432. Weber, J. W., Calado, V. E. & van de Sanden, M. C. M. Optical constants of graphene measured by spectroscopic ellipsometry. *Applied Physics Letters* **97**, https://doi.org/10.1063/1.3475393 (2010).
433. Weiting, F. & Yixun, Y. Temperature effects on the refractive index of lead telluride and zinc selenide. *Infrared Physics* **30**, 371–373, https://doi.org/10.1016/0020-0891(90)90055-z (1990).
434. Werner, W. S. M., Glantschnig, K. & Ambrosch-Draxl, C. Optical constants and inelastic electron-scattering data for 17 elemental metals. *Journal of Physical and Chemical Reference Data* **38**, 1013–1092, https://doi.org/10.1063/1.3243762 (2009).
435. Werner, K. *et al*. Ultrafast mid-infrared high harmonic and supercontinuum generation with n_2 characterization in zinc selenide. *Optics Express* **27**, 2867, https://doi.org/10.1364/oe.27.002867 (2019).
436. Wettling, W. & Windscheif, J. Elastic constants and refractive index of boron phosphide. *Solid State Communications* **50**, 33–34, https://doi.org/10.1016/0038-1098(84)90053-x (1984).
437. Whang, U. S., Arakawa, E. T. & Callcott, T. A. Optical properties of Cs for photons of energy 36–96 eV. *Journal of the Optical Society of America* **61**, 740, https://doi.org/10.1364/josa.61.000740 (1971).
438. Whang, U. S., Arakawa, E. T. & Callcott, T. A. Optical properties of K between 4 and 10.7 eV and comparison with Na, Rb, and Cs. *Physical Review B* **6**, 2109–2118, https://doi.org/10.1103/physrevb.6.2109 (1972).
439. Whang, U. S., Arakawa, E. T. & Callcott, T. A. Optical properties of Rb between 3.3 and 10.5 eV. *Physical Review B* **5**, 2118–2124, https://doi.org/10.1103/physrevb.5.2118 (1972).
440. White, W. T., Smith, W. L. & Milam, D. Direct measurement of the nonlinear refractive-index coefficient γ at 355 nm in fused silica and in BK-10 glass. *Optics Letters* **9**, 10, https://doi.org/10.1364/ol.9.000010 (1984).
441. Williams, P. A. *et al*. Optical, thermo-optic, electro-optic, and photoelastic properties of bismuth germanate ($Bi_4Ge_3O_{12}$). *Applied Optics* **35**, 3562, https://doi.org/10.1364/ao.35.003562 (1996).
442. Windt, D. L. *et al*. Optical constants for thin films of Ti, Zr, Nb, Mo, Ru, Rh, Pd, Ag, Hf, Ta, W, Re, Ir, Os, Pt, and Au from 24 Å to 1216 Å. *Applied Optics* **27**, 246, https://doi.org/10.1364/ao.27.000246 (1988).
443. Wood, D. L. & Nassau, K. Refractive index of cubic zirconia stabilized with yttria. *Applied Optics* **21**, 2978, https://doi.org/10.1364/ao.21.002978 (1982).
444. Wood, D. L., Nassau, K., Kometani, T. Y. & Nash, D. L. Optical properties of cubic hafnia stabilized with yttria. *Applied Optics* **29**, 604, https://doi.org/10.1364/ao.29.000604 (1990).
445. Woods, B. W., Payne, S. A., Marion, J. E., Hughes, R. S. & Davis, L. E. Thermomechanical and thermo-optical properties of the $LiCaAlF_6:Cr^{3+}$ laser material. *Journal of the Optical Society of America B* **8**, 970, https://doi.org/10.1364/josab.8.000970 (1991).
446. Wu, S.-T. Refractive index dispersions of liquid crystals. *Optical Engineering* **32**, 1775, https://doi.org/10.1117/12.143988 (1993).
447. Wu, Y. *et al*. Intrinsic optical properties and enhanced plasmonic response of epitaxial silver. *Advanced Materials* **26**, 6106–6110, https://doi.org/10.1002/adma.201401474 (2014).
448. Yakubovsky, D. I., Arsenin, A. V., Stebunov, Y. V., Fedyanin, D. Y. & Volkov, V. S. Optical constants and structural properties of thin gold films. *Optics Express* **25**, 25574, https://doi.org/10.1364/oe.25.025574 (2017).
449. Yakubovsky, D. I. *et al*. Ultrathin and ultrasmooth gold films on monolayer MoS_2. *Advanced Materials Interfaces* **6**, https://doi.org/10.1002/admi.201900196 (2019).
450. Yamaguchi, S. & Hanyu, T. Optical properties of potassium. *Journal of the Physical Society of Japan* **31**, 1431–1441, https://doi.org/10.1143/jpsj.31.1431 (1971).
451. Yamaguchi, S. & Hanyu, T. The optical properties of Rb. *Journal of the Physical Society of Japan* **35**, 1371–1377, https://doi.org/10.1143/jpsj.35.1371 (1973).
452. Yang, H. U. *et al*. Optical dielectric function of silver. *Physical Review B* **91**, https://doi.org/10.1103/physrevb.91.235137 (2015).
453. Yao, C., Shen, W., Hu, X. & Hu, C. Optical properties of large-size and damage-free polished Lu_2O_3 single crystal covering the ultraviolet-visible-and near-infrared (UV–VIS–NIR) spectral region. *Journal of Alloys and Compounds* **897**, 162726, https://doi.org/10.1016/j.jallcom.2021.162726 (2022).
454. Yim, C. *et al*. Investigation of the optical properties of MoS_2 thin films using spectroscopic ellipsometry. *Applied Physics Letters* **104**, 103114, https://doi.org/10.1063/1.4868108 (2014).
455. Zahedpour, S., Wahlstrand, J. K. & Milchberg, H. M. Measurement of the nonlinear refractive index of air constituents at mid-infrared wavelengths. *Optics Letters* **40**, 5794, https://doi.org/10.1364/ol.40.005794 (2015).
456. Zelmon, D. E., Small, D. L. & Jundt, D. Infrared corrected Sellmeier coefficients for congruently grown lithium niobate and 5 mol% magnesium oxide-doped lithium niobate. *Journal of the Optical Society of America B* **14**, 3319, https://doi.org/10.1364/josab.14.003319 (1997).

457. Zelmon, D. E., Small, D. L. & Page, R. Refractive-index measurements of undoped yttrium aluminum garnet from 04 to 50 μm. *Applied Optics* **37**, 4933, https://doi.org/10.1364/ao.37.004933 (1998).
458. Zelmon, D. E., Hanning, E. A. & Schunemann, P. G. Refractive-index measurements and Sellmeier coefficients for zinc germanium phosphide from 2 to 9 μm with implications for phase matching in optical frequency-conversion devices. *Journal of the Optical Society of America B* **18**, 1307, https://doi.org/10.1364/josab.18.001307 (2001).
459. Zelmon, D. E., Bayya, S. S., Sanghera, J. S. & Aggarwal, I. D. Dispersion of barium gallogermanate glass. *Applied Optics* **41**, 1366, https://doi.org/10.1364/ao.41.001366 (2002).
460. Zemel, J. N., Jensen, J. D. & Schoolar, R. B. Electrical and optical properties of epitaxial films of PbS, PbSe, PbTe, and SnTe. *Physical Review* **140**, A330–A342, https://doi.org/10.1103/physrev.140.a330 (1965).
461. Zernike, F. Refractive indices of ammonium dihydrogen phosphate and potassium dihydrogen phosphate between 2000 Å and 15 μ. *Journal of the Optical Society of America* **54**, 1215, https://doi.org/10.1364/josa.54.001215 (1964).
462. Zhang, Z. M., Lefever-Button, G. & Powell, F. R. Infrared refractive index and extinction coefficient of polyimide films. *International Journal of Thermophysics* **19**, 905–916, https://doi.org/10.1023/a:1022655309574 (1998).
463. Zhang, D., Kong, Y. & Zhang, J.-Y. Optical parametric properties of 532-nm-pumped beta-barium-borate near the infrared absorption edge. *Optics Communications* **184**, 485–491, https://doi.org/10.1016/s0030-4018(00)00968-8 (2000).
464. Zhang, J., Lu, Z. H. & Wang, L. J. Precision refractive index measurements of air, N_2, O_2, Ar, and CO_2 with a frequency comb. *Applied Optics* **47**, 3143, https://doi.org/10.1364/ao.47.003143 (2008).
465. Zhang, H. *et al*. Measuring the refractive index of highly crystalline monolayer MoS_2 with high confidence. *Scientific Reports* **5**, https://doi.org/10.1038/srep08440 (2015).
466. Zhang, X., Qiu, J., Li, X., Zhao, J. & Liu, L. Complex refractive indices measurements of polymers in visible and near-infrared bands. *Applied Optics* **59**, 2337, https://doi.org/10.1364/ao.383831 (2020).
467. Zhang, X., Qiu, J., Zhao, J., Li, X. & Liu, L. Complex refractive indices measurements of polymers in infrared bands. *Journal of Quantitative Spectroscopy and Radiative Transfer* **252**, 107063, https://doi.org/10.1016/j.jqsrt.2020.107063 (2020).
468. Zhang, X. *et al*. Optimizing the design of the vapor-deposited $CsPbCl_3$-based optoelectronic devices via simulations and experiments. *Advanced Functional Materials* 2310945, https://doi.org/10.1002/adfm.202310945 (2023).
469. Zheng, Q., Wang, X. & Thompson, D. Temperature-dependent optical properties of monocrystalline CaF_2, BaF_2, and MgF_2. *Optical Materials Express* **13**, 2380, https://doi.org/10.1364/ome.496246 (2023).
470. Zhukovsky, S. V. *et al*. Experimental demonstration of effective medium approximation breakdown in deeply subwavelength all-dielectric multilayers. *Physical Review Letters* **115**, https://doi.org/10.1103/physrevlett.115.177402 (2015).
471. Zollner, S., Lin, C., Schönherr, E., Böhringer, A. & Cardona, M. The dielectric function of AlSb from 1.4 to 5.8 eV determined by spectroscopic ellipsometry. *Journal of Applied Physics* **66**, 383–387, https://doi.org/10.1063/1.343888 (1989).

Acknowledgements

The development of the n_2 segment of the *refractiveindex.info* database was facilitated by grants from the US Department of Energy Accelerator Stewardship Program. Originally a part of the Office of High Energy Physics (HEP), this program is now under the purview of the Accelerator Research & Development and Production (ARDAP) office. The author extends heartfelt appreciation to the multitude of contributors from the scientific and engineering realms. Their contributions, spanning data submissions, error reporting, and invaluable insights, have been instrumental in the refinement and expansion of the database. The collective engagement of this dedicated community has been pivotal in elevating the database to its current stature of utility and comprehensiveness.

Author contributions

M.N.P. conceptualized, created, and has maintained the *refractiveindex.info* database throughout the years, ensuring its continuous update and improvement to meet the evolving needs of the optics and photonics community. The compilation, verification, and organization of the data, as well as the development and maintenance of the associated tools included with the database, were all carried out by M.N.P. The invaluable feedback and data contributions from the user community have played a crucial role in enhancing the comprehensiveness and accuracy of the database.

Competing interests

The author declares no competing interests. However, for complete transparency, it is noted that the author is the owner of the RefractiveIndex.INFO website, which utilizes the *refractiveindex.info* database to provide optical constants. The website generates modest revenue from advertisements, which primarily covers maintenance expenses including web hosting, domain registration, and email services.

Additional information

Correspondence and requests for materials should be addressed to M.N.P.